# Patatin-Related Phospholipase pPLAIIIδ Increases Seed Oil Content with Long-Chain Fatty Acids in Arabidopsis[1][C][W][OA]

**Maoyin Li, Sung Chul Bahn, Chuchuan Fan, Jia Li, Tien Phan, Michael Ortiz, Mary R. Roth, Ruth Welti, Jan Jaworski, and Xuemin Wang***

Department of Biology, University of Missouri, St. Louis, Missouri 63121 (M.L., S.C.B., T.P., X.W.); Donald Danforth Plant Science Center, St. Louis, Missouri 63132 (M.L., S.C.B., J.L., M.O., J.J., X.W.); National Key Laboratory of Crop Genetic Improvement, Huazhong Agricultural University, Wuhan 430070, China (C.F.); and Kansas Lipidomics Research Center, Division of Biology, Kansas State University, Manhattan, Kansas 66506 (M.R.R., R.W.)

The release of fatty acids from membrane lipids has been implicated in various metabolic and physiological processes, but in many cases, the enzymes involved and their functions in plants remain unclear. Patatin-related phospholipase As (pPLAs) constitute a major family of acyl-hydrolyzing enzymes in plants. Here, we show that pPLAIIIδ promotes the production of triacylglycerols with 20- and 22-carbon fatty acids in Arabidopsis (*Arabidopsis thaliana*). Of the four pPLAIIIs (α, β, γ, δ), only *pPLAIIIδ* gene knockout results in a decrease in seed oil content, and *pPLAIIIδ* is most highly expressed in developing embryos. The overexpression of *pPLAIIIδ* increases the content of triacylglycerol and 20- and 22-carbon fatty acids in seeds with a corresponding decrease in 18-carbon fatty acids. Several genes in the glycerolipid biosynthetic pathways are up-regulated in *pPLAIIIδ*-overexpressing siliques. pPLAIIIδ hydrolyzes phosphatidylcholine and also acyl-coenzyme A to release fatty acids. *pPLAIIIδ*-overexpressing plants have a lower level, whereas *pPLAIIIδ* knockout plants have a higher level, of acyl-coenzyme A than the wild type. Whereas seed yield decreases in transgenic plants that ubiquitously overexpress *pPLAIIIδ*, seed-specific overexpression of *pPLAIIIδ* increases seed oil content without any detrimental effect on overall seed yield. These results indicate that pPLAIIIδ-mediated phospholipid turnover plays a role in fatty acid remodeling and glycerolipid production.

Lipids play essential structural, metabolic, and regulatory roles in plant growth, development, and stress responses. In addition, plant lipids are a major source of food and renewable materials for various industrial and energy applications (Dyer et al., 2008; Hayden et al., 2011; Rogalski and Carrer, 2011; Bates and Browse, 2012). Substantial progress has been made toward a basic understanding of the biochemical reactions of lipid biosynthesis in plants, but many fundamental questions about lipid metabolism remain unanswered (Weselake et al., 2009; Chapman and Ohlrogge, 2012). Recent results suggest that the metabolism of phosphatidylcholine (PC) plays multiple important roles in glycerolipid production. An increasing line of research shows that storage lipid triacylglycerols (TAGs) are not synthesized primarily via the Kennedy pathway but are derived from PC through acyl editing (Bates et al., 2009, 2012; Tjellström et al., 2012). PC is also hypothesized to be involved in the trafficking of fatty acids from the plastid to the endoplasmic reticulum (ER), where glycerolipids, including TAG, are assembled (Wang and Benning, 2012). It is proposed that plastidial fatty acids are transferred to lysophosphatidylcholine (LPC) to form PC, which serves as a substrate for fatty acid desaturation and modification. While the importance of PC metabolism in TAG production is clear, the specific enzymes involved in PC turnover are not well elucidated (Bates et al., 2012; Chapman and Ohlrogge, 2012), and the impact of PC turnover on TAG accumulation remains to be determined.

Phospholipase A (PLA) hydrolyzes PC to produce LPC and a free fatty acid (FFA). This reaction has been

[1] This work was supported by the U.S. Department of Energy, Office of Science, Office of Basic Energy Sciences (grant no. DE–SC0001295 to J.L., J.J., and X.W.), by the National Science Foundation (grant no. MCB–0922879 to M.L., S.B., T.P., and M.O.), and by the National Natural Science Foundation of China (grant no. 30900787 to C.F.). Instrument acquisition and method development at the Kansas Lipidomics Research Center were supported by the National Science Foundation (grant nos. MCB–0920663 and DBI–0521587 to R.W.) and by the Kansas Experimental Program to Stimulate Competitive Research (award no. EPS–0236913 subaward to X.W. and R.W.).

* Corresponding author; e-mail swang@danforthcenter.org.

The author responsible for distribution of materials integral to the findings presented in this article in accordance with the policy described in the Instructions for Authors (www.plantphysiol.org) is: Xuemin Wang (swang@danforthcenter.org).

[C] Some figures in this article are displayed in color online but in black and white in the print edition.

[W] The online version of this article contains Web-only data.

[OA] Open Access articles can be viewed online without a subscription.

www.plantphysiol.org/cgi/doi/10.1104/pp.113.216994

  

implicated in various cellular functions, including the production of lipid mediators, carbon partitioning, and cell elongation. Patatin-containing PLA (pPLA) is a major family of intracellular acyl-hydrolyzing enzymes in plants (Scherer et al., 2010; Murakami et al., 2011). The 10-gene pPLA family in Arabidopsis (*Arabidopsis thaliana*) is grouped into three subfamilies, pPLAI, pPLAII ($\alpha$, $\beta$, $\gamma$, $\delta$, $\varepsilon$), and pPLAIII ($\alpha$, $\beta$, $\gamma$, $\delta$). pPLAI has been shown to contribute to resistance to *Botrytis cinerea*, possibly by mediating the basal levels of jasmonate production (Yang et al., 2007), whereas pPLAII$\alpha$ negatively modulates both plant response to bacterial pathogens (La Camera et al., 2005) and oxylipin production (Yang et al., 2012). pPLAII$\beta$ impacts root elongation during phosphate deficiency, and pPLAII$\gamma$ and pPLAII$\delta$ have been implicated in involvement in auxin responses (Rietz et al., 2004, 2010). Activation tagging of pPLAIII$\delta$ and overexpression (OE) of pPLAIII$\beta$ resulted in decreased cell elongation and stunted growth (Huang et al., 2001; Li et al., 2011). These results indicate that the pPLA family plays important, diverse roles in plant growth and stress responses, but their role in seed oil production is not known.

One enigma from recent genomic analysis of Arabidopsis has been that there are as many genes annotated as being involved in lipid catabolism as there are in lipid synthesis (Li-Beisson et al., 2010). While the functions for many genes involved in lipid biosynthesis have been documented, little is known about the role of lipid-hydrolyzing enzymes in lipid metabolism

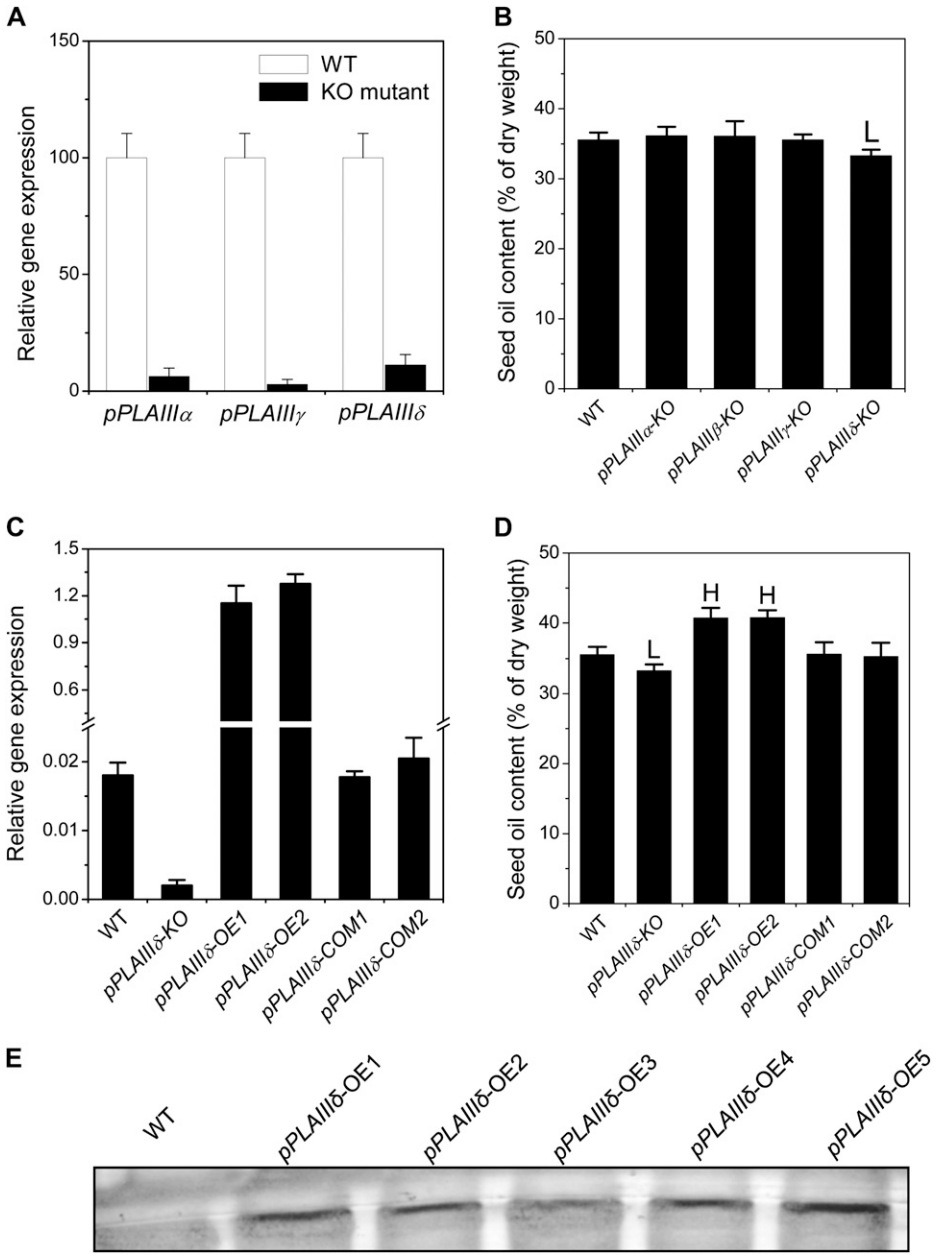


**Figure 1.** Alterations of pPLAIII$\delta$ change Arabidopsis seed oil content. A, Transcript levels of *pPLAIII$\alpha$*, *pPLAIII$\gamma$*, and *pPLAIII$\delta$* in 2-week-old rosettes. The RNA levels were determined by real-time PCR and normalized to the level of the wild type (WT). Values are means ± SE ($n$ = 3). B, Seed oil content in T-DNA insertion mutants of *pPLAIII$\alpha$-KO*, *pPLAIII$\beta$-KO*, *pPLAIII$\gamma$-KO*, and *pPLAIII$\delta$-KO*. Values are means ± SE ($n$ = 3). $^{L}$Significantly lower at $P < 0.05$ compared with the wild type, based on Student's $t$ test. C, Transcript levels of *pPLAIII$\delta$* in wild-type, *pPLAIII$\delta$* KO, OE, and COM plants. *pPLAIII$\delta$-OE1*, *pPLAIII$\delta$-OE2*, *pPLAIII$\delta$-COM1*, and *pPLAIII$\delta$-COM2* are independent lines of the T3 generation of *pPLAIII$\delta$-OE* and *pPLAIII$\delta$-COM*. The RNA levels were determined by real-time PCR and normalized in comparison with *UBQ10*. Values are means ± SE ($n$ = 3). D, Seed oil content in *pPLAIII$\delta$-OE* and *pPLAIII$\delta$-COM* T3 seeds. *pPLAIII$\delta$* expression in OE lines was under the control of the cauliflower mosaic virus 35S promoter, while in the COM lines, it was under the control of its own promoter. Values are means ± SE ($n$ = 3). $^{H}$Significantly higher and $^{L}$significantly lower, each at $P < 0.05$ compared with the wild type, based on Student's $t$ test. E, Immunoblotting of GFP-tagged pPLAIII$\delta$ in Arabidopsis. Leaf proteins extracted from plants were separated by 8% SDS-PAGE, transferred to a polyvinylidene difluoride membrane, and visualized with alkaline phosphatase conjugated to a secondary anti-mouse antibody after blotting with GFP antibody. Five independent T3 lines of *pPLAIII$\delta$-OE* mutants were examined.

and oil production. A recent study compared the transcriptomes of mesocarp from oil palm (*Elaeis guineensis* 'Jacq') and date palm (*Phoenix dactylifera*) that accumulate approximately 90% and 1% oil, respectively (Bourgis et al., 2011). The mRNA level of key genes in fatty acid synthesis in oil palm mesocarp is 2- to 44-fold higher than in date palm. The mRNA level of palm pPLAIII$\beta$ is 22-fold higher in oil palm compared with date palm mesocarp (Bourgis et al., 2011), but the role for pPLAIII in oil accumulation remains to be determined. Patatin-related enzymes typically contain a catalytic center with the esterase box GXSXG and other specific motifs including a catalytic dyad motif, which typically contains Asp-Gly-Gly (Scherer et al., 2010). The pPLAIII subfamily differs from pPLAI and pPLAII in that it does not contain the canonical esterase GXSXG motif but instead has the sequence GXGXG (Scherer et al., 2010). Our recent analysis of *pPLAIII$\beta$* shows that pPLAIII$\beta$ hydrolyzes PC to produce LPC and FFAs (Li et al., 2011). Moreover, OE of *pPLAIII$\beta$* increases membrane glycerolipid content in vegetative tissues, whereas its gene knockout (KO) has the opposite effect. These observations prompted us to determine the role of *pPLAIIIs* in seed oil production. Here, we show that pPLAIII$\delta$ promotes TAG production with increased accumulation of long-chain fatty acids in Arabidopsis seeds.

## RESULTS

### pPLAIII$\delta$ Increases Seed Oil Content

To investigate the function of pPLAIIIs in seed oil production, we isolated transfer DNA (T-DNA) insertional KO mutants for all four pPLAIIIs (Supplemental Fig. S1). The T-DNA insertion sites of *pPLAIII$\alpha$* and *pPLAIII$\beta$* are in the first exon, while the insertion sites of *pPLAIII$\gamma$* and *pPLAIII$\delta$* locate in the 5′ untranslated region (Supplemental Fig. S1B). All of these insertional mutants have a negligible level of transcript as measured by real-time PCR of *pPLAIII$\alpha$*, *pPLAIII$\gamma$*, and *pPLAIII$\delta$* (Fig. 1A). The loss of *pPLAIII$\beta$* expression in *pPLAIII$\beta$-KO* was described previously (Li et al., 2011). However, only the *pPLAIII$\delta$-KO* seeds, not the other pPLAIIIs, displayed a significant change in oil content compared with wild-type seeds; the oil contents of *pPLAIII$\delta$-KO* and wild-type seeds were 33% and 35.5% of the seed weight, respectively (Fig. 1B). To confirm the effect of *pPLAIII$\delta$* on seed oil production, we genetically complemented the KO by transferring *pPLAIII$\delta$* with its native promoter and terminator sequences into the KO mutant (designated as COM; Supplemental Fig. S1C). Expression of *pPLAIII$\delta$* in the COM lines was restored to the wild-type level (Fig. 1C), and the oil content in COM seeds was the same as that of the wild type (Fig. 1D).

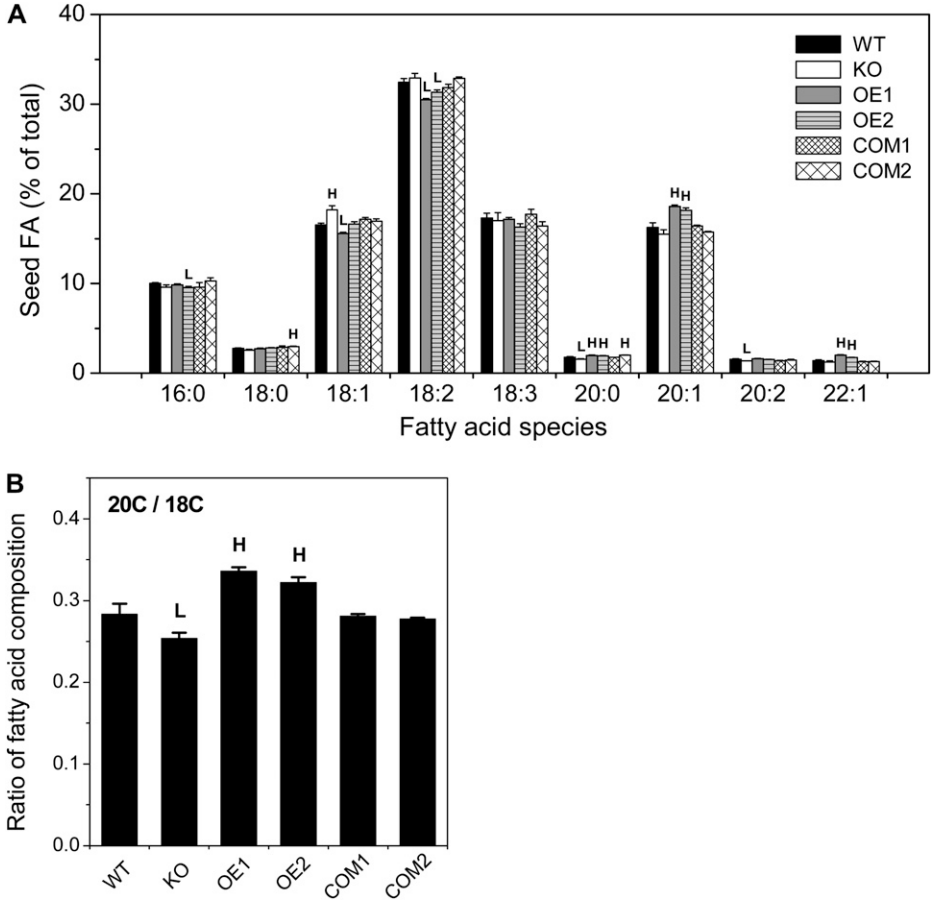


**Figure 2.** pPLAIII$\delta$ increases 20C fatty acid content at the expense of 18C fatty acids. A, Fatty acid (FA) compositions of *pPLAIII$\delta$* KO, OE, COM, and wild-type (WT) seeds. Values are means ± SE ($n$ = 3). $^{H}$Significantly higher and $^{L}$significantly lower, each at $P < 0.05$ compared with the wild type, based on Student's $t$ test. B, 20C/18C ratio in *pPLAIII$\delta$* KO, OE, COM, and wild-type seeds. 20C/18C denotes fatty acids with 20 carbons over fatty acids with 18 carbons. Values are means ± SE ($n$ = 3). $^{H}$Significantly higher and $^{L}$significantly lower, each at $P < 0.05$ compared with the wild type, based on Student's $t$ test.

Analysis of mRNA accumulation patterns for pPLAIIIs in seeds indicates that *pPLAIIIα*, *pPLAIIIβ*, and *pPLAIIIγ* were expressed in tissues that do not accumulate large amounts of TAG in developing seeds (Supplemental Fig. S2, A–E). In mature green seeds, *pPLAIIIγ* was expressed mostly in seed coat, *pPLAIIIβ* mostly in chalazal seed coat, and *pPLAIIIα* mostly in seed coats and peripheral endosperm (Supplemental Fig. S2, C–E). In contrast, *pPLAIIIδ* was expressed in developing radicle and in cotyledons, the major storage tissue for seed oil in Arabidopsis (Supplemental Fig. S2F). The mRNA accumulation pattern of the pPLAIII genes is consistent with a *pPLAIIIδ*-specific effect on seed oil content; thus, further analysis was focused on *pPLAIIIδ*.

To further investigate pPLAIIIδ function, we produced multiple OE Arabidopsis lines by placing *pPLAIIIδ* under the control of cauliflower mosaic virus 35S promoter (*35S::pPLAIIIδ-OE*; Supplemental Fig. S1C). The mRNA level of pPLAIIIδ was increased substantially in OE over wild-type plants (Fig. 1C). The presence of the introduced GFP-tagged pPLAIIIδ was detected by immunoblotting with a GFP antibody (Fig. 1E). Seed oil content in two OE lines was approximately 40.5%, which was 5% higher than that of the wild type (35.5%; Fig. 1D). Taken together, these data indicate that pPLAIIIδ plays a positive role in seed oil accumulation.

### pPLAIIIδ Increases 20-Carbon Fatty Acid Content at the Expense of 18-Carbon Fatty Acids

The fatty acid composition was significantly altered in *pPLAIIIδ-KO* and *35S::pPLAIIIδ-OE* seeds (Fig. 2A). The levels of 18-carbon fatty acids tended to increase in KO and decrease in OE seeds compared with the wild type. For example, 18:1 was increased by 10% in KO but decreased 6% in OE1. Conversely, the amounts of 20-carbon fatty acids 20:0 and 20:2 were decreased by

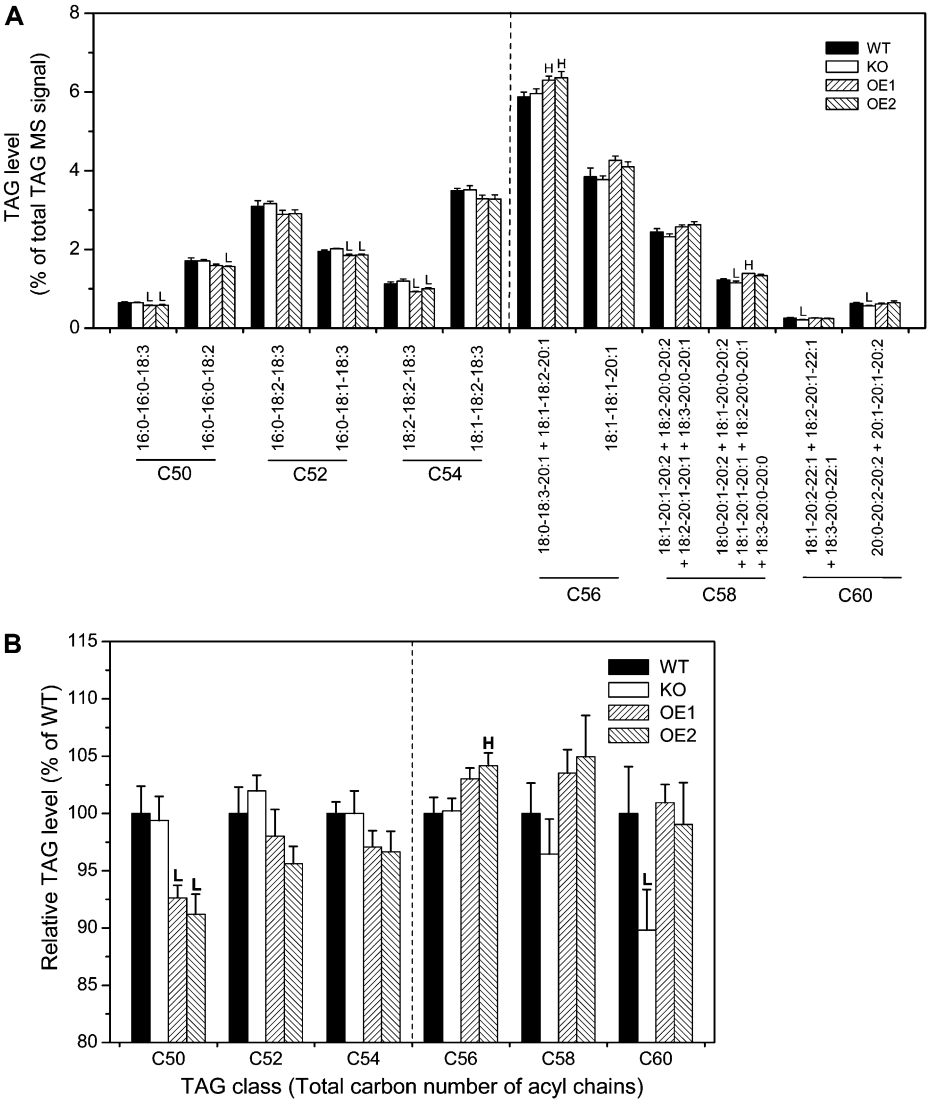


**Figure 3.** pPLAIIIδ promotes the accumulation of 20C-containing TAG species. A, Normalized mass spectra (as a percentage of the total) from TAG species with the indicated fatty acyl combinations in wild-type, KO, and OE seeds. The fatty acids making up each molecular species are indicated, but no positional specificity is implied. The TAG species shown on the left side of the dashed lines contain only 16- and 18-carbon chains, while those on the right include one or more 20-carbon chains. Values are means ± SE ($n = 5$). $^{H}$Significantly higher and $^{L}$significantly lower, each at $P < 0.05$ compared with the wild type, based on Student's *t* test. B, Normalized mass spectra (as a percentage of the wild type) from TAGs, grouped by total acyl carbons, were classified as C50, C52, C54, C56, C58, and C60. The major components in C50, C52, and C54 are 18C fatty acyl-containing TAGs, while C56, C58, and C60 are TAGs containing one or more 20C fatty acyl-containing TAGs. Values are means ± SE ($n = 5$). $^{H}$Significantly higher and $^{L}$significantly lower, each at $P < 0.05$ compared with the wild type, based on Student's *t* test.

12% and 12% in KO, while 20:0 and 20:1 were increased by 12% and 15% in OE lines, compared with the wild type. The 22-carbon species, 22:1, showed a trend similar to the 20-carbon species. The ratio of 20- to 18-carbon fatty acids was decreased by 10% in KO and increased by 19% in OE compared with the wild type (Fig. 2B). The fatty acid composition in COM seeds was similar to that of wild-type seeds (Fig. 2B). Thus, the increased mRNA level of *pPLAIIIδ* promoted the accumulation of longer chain fatty acids at the expense of 18-carbon fatty acids, 18:1 and 18:2, whereas *pPLAIIIδ-KO* decreased the production of longer chains with increased accumulation of 18-carbon fatty acids.

Fatty acids in Arabidopsis seeds occur primarily in esterified form in TAGs. TAGs include many different molecular species with varied carbon chain lengths and degrees of unsaturation in the three acyl chains. Three acyl chains in TAG are not randomly distributed. Since pPLAIIIδ affects 18:1 and 20:1 accumulation in TAG, we wondered if pPLAIIIδ alters the distribution of three acyl chains and thus produces some unique TAG molecule species. Therefore, we analyzed the TAG species in wild-type, KO, and OE seeds by electrospray ionization-tandem mass spectrometry (ESI-MS/MS). The major fatty acyl chain carbon numbers (C) in seed TAGs are 16C, 18C, and 20C, and the major TAG species have total C of C50 (e.g. 16-16-18), C52 (e.g. 16-18-18), C54 (e.g. 18-18-18), C56 (e.g. 18-18-20), C58 (e.g. 18-20-20), and C60 (e.g. 20-20-20; Fig. 3). The percentages of C50, C52, and C54 TAG species in total TAGs, as indicated by their relative mass spectral signals, tended to be higher in KO and lower in OE mutants when compared with the wild type, while the levels of C56, C58, and C60 TAG species were changed in the opposite manner in KO and OE lines of *pPLAIIIδ* (Fig. 3; Supplemental Fig. S3). For example, the percentages of some 16C- and 18C-containing TAGs (16:0-16:0-18:3, 16:0-18:1-18:3, 18:2-18:2-18:3) were significantly lower in OE mutants than in the wild type (Fig. 3A). While certain TAG species could not be quantified individually, and thus their compositional percentages were expressed in combination, the percentages of 20C-containing TAGs and TAG groups tended to be or were significantly lower in KO and higher in OE mutants compared with the wild type (Fig. 3A). Overall, the relative amounts of C50, C52, and C54 TAGs tended to be lower, while C56, C58, and C60 TAGs tended to be higher in OE mutant seeds compared with the wild type (Fig. 3B). Measurement of 113 additional TAG species and eight TAG species groups confirmed the trend for the percentages of 18C-containing TAGs to be lower and the 20C-containing TAGs to be higher in OE lines compared with the wild type (Supplemental Fig. S3, A–E). Taken together, these data indicate that pPLAIIIδ promotes the accumulation of 20C-containing TAG species.

### pPLAIIIδ-OE Increases the Transcript Levels of Genes in TAG and PC Synthesis

To gain insight into how pPLAIIIδ facilitates TAG accumulation and modification, we measured the mRNA levels of selected genes in TAG and PC synthesis and metabolism in developing Arabidopsis siliques (Fig. 4). In the Kennedy pathway of TAG

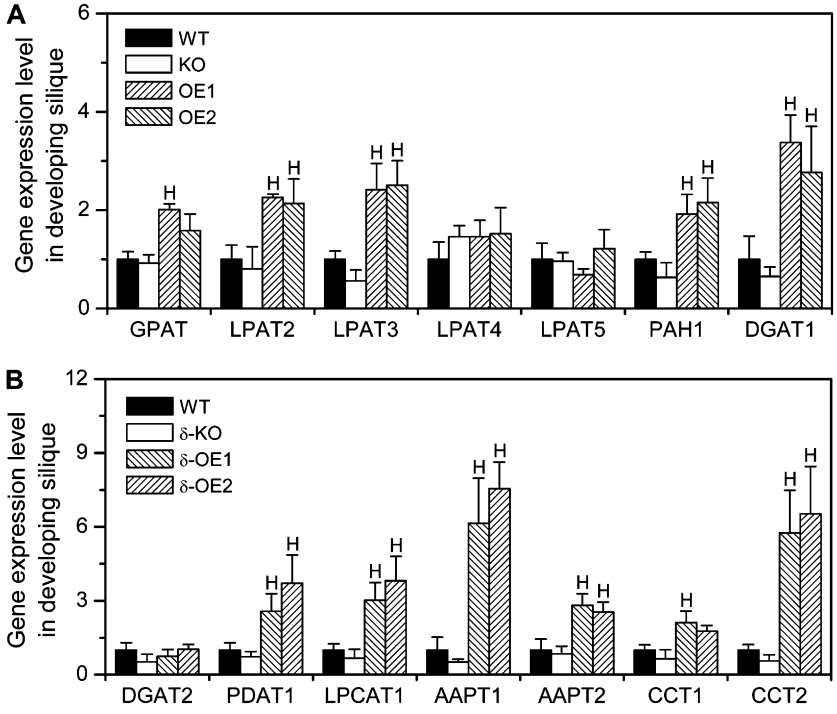


**Figure 4.** pPLAIIIδ increases the RNA levels of genes in TAG and PC synthesis in siliques. RNA levels were determined by real-time PCR and normalized in comparison with *UBQ10*. Values are means ± SE ($n$ = 3 technical replicates). $^{H}$Significantly higher at $P < 0.05$ compared with the wild type, based on Student's $t$ test. WT, Wild type.

biosynthesis, glycerol-3-P is sequentially acylated by glycerol phosphate acyltransferase (GPAT) and lysophosphatidic acid acyltransferase (LPAT), followed by phosphatidic acid phosphohydrolase (PAH) and diacylglycerol acyltransferase (DGAT). The transcript levels for the genes in the Kennedy pathway, including *GPAT*, *LPAT2*, *LPAT3*, *PAH*, and *DGAT1*, were increased 2- to 5-fold in *pPLAIIIδ-OE* lines (Fig. 4A). By comparison, mRNA levels of both *DGAT2* and *LPAT5* were the same in wild-type, *pPLAIIIδ-KO*, and *35S*::*pPLAIIIδ-OE* siliques (Fig. 4). Phospholipid:diacylglycerol acyltransferase (PDAT) catalyzes the transfer of a fatty acid from PC to diacylglycerol (DAG) to produce TAG. The mRNA level of *PDAT1* was increased by almost 3-fold in OE lines compared with the wild type (Fig. 4B).

In the Kennedy pathway of PC biosynthesis, choline phosphate:CTP cytidylyltransferase (CCT) synthesizes CDP-choline using CTP and phosphocholine, and aminoalcohol-phosphotransferase (AAPT) catalyzes the last step of PC synthesis by transferring phosphocholine to DAG from CDP-choline. There are two CCTs and AAPTs in Arabidopsis. Compared with the wild type, the mRNA levels of *CCT2* and *AAPT1* were increased almost by 10-fold, whereas the increase in *CCT1* and *AAPT2* was about 2-fold in *pPLAIIIδ-OE* siliques (Fig. 4B). The mRNA abundance of *Lysophosphatidylcholine: acyl-coenzyme A acyltransferase1* (*LPCAT1*) was also increased 3-fold in OE lines (Fig. 4B). These data demonstrate that OE of *pPLAIIIδ* increases the mRNA levels of genes involved in TAG and PC synthesis. On the other hand, in KO siliques, the mRNA levels for the lipid-metabolizing genes were not significantly different from that of the wild type, even though the mRNA levels for several of these genes tended to be lower than that of the wild type (Fig. 4). These results suggest that the loss of *pPLAIIIδ* may be partially compensated for by other pPLAs.

### pPLAIIIδ Hydrolyzes PC and Acyl-CoA and Affects Acyl-CoA Levels in Arabidopsis

pPLAIIIδ is more distantly related to the other three pPLAIIIs than they are to each other (Supplemental Fig. S1A). pPLAIIIδ has an Asp in the Asp-Gly-Gly catalytic dyad motif, similar to pPLAs in the other groups, whereas in pPLAIIIβ and pPLAIIIγ, the Asp is replaced by Gly (Li et al., 2011). To determine the enzymatic function of pPLAIIIδ, we expressed 6×His-tagged pPLAIIIδ in *Escherichia coli* and purified it to near homogeneity (Fig. 5A). The PC-hydrolyzing activity of pPLAIIIδ was examined because PC is the most abundant phospholipid and serves as a key intermediate for TAG synthesis. Incubation of pPLAIIIδ with 16:0-18:2-PC resulted in the production of FFA and LPC. pPLAIIIδ hydrolysis at the *sn*-1 position produces 16:0-FFA and 18:2-LPC (Fig. 5B), whereas pPLAIIIδ hydrolysis at the *sn*-2 position produces 18:2-FFA and 16:0-LPC (Fig. 5C). The production of 18:2-FFA was approximately 5-fold more than that of 16:0-FFA, and correspondingly, much more 16:0-LPC was formed than 18:2-LPC. These data indicate that pPLAIIIδ hydrolyzes PC at both the *sn*-1 and *sn*-2 positions and that pPLAIIIδ preferentially releases 18:2 from the *sn*-2 position.

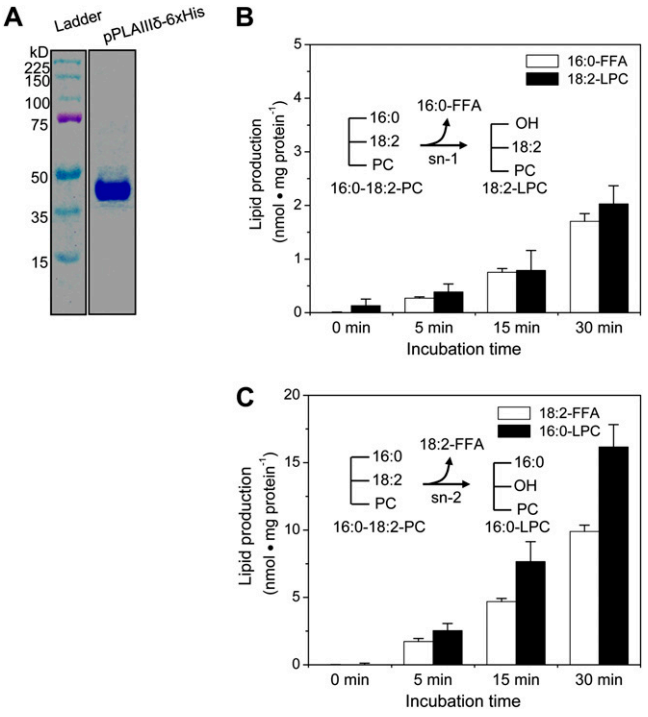


**Figure 5.** pPLAIIIδ was purified and hydrolyzes PC at the *sn*-1 and *sn*-2 positions. A, Coomassie blue staining of an 8% SDS-PAGE gel loaded with affinity-purified pPLAIIIδ-6×His from *E. coli*. B, Production of 16:0-FFA and 18:2-LPC from hydrolysis of 16:0-18:2 PC at the *sn*-1 position (inset). Values are means ± SE ($n = 3$ separate samples). C, Production of 18:2-FFA and 16:0-LPC from hydrolysis of 16:0-18:2 PC at the *sn*-2 position (inset). Values are means ± SE ($n = 3$). [See online article for color version of this figure.]

In addition, we determined whether pPLAIIIδ could hydrolyze acyl-CoA, because our previous study showed that another pPLAIII member, pPLAIIIβ, has thioesterase activity (Li et al., 2011). Incubation of pPLAIIIδ with 18:3-CoA resulted in the steady production of 18:3-FFA with increasing reaction time (Fig. 6A), indicating that pPLAIIIδ possesses a thioesterase activity. We then determined whether the alterations of *pPLAIIIδ* expression impacted the acyl-CoA content in Arabidopsis. In siliques that included developing seeds with active storage lipid biosynthesis, the level of total acyl-CoA was 19% higher in KO and 18% lower in OE mutants than in the wild type (Fig. 6B). The major acyl-CoA species are 18:3-CoA and 18:2-CoA, followed by 16:0-CoA. The levels of 18:1-CoA, 18:2-CoA, and 18:3-CoA were significantly higher in KO, and the levels of 16:0-CoA and 18:2-CoA were significantly lower in OE, than in wild-type siliques (Fig. 6C). These data are consistent with pPLAIIIδ functioning as an acyl-CoA thioesterase activity in vivo.

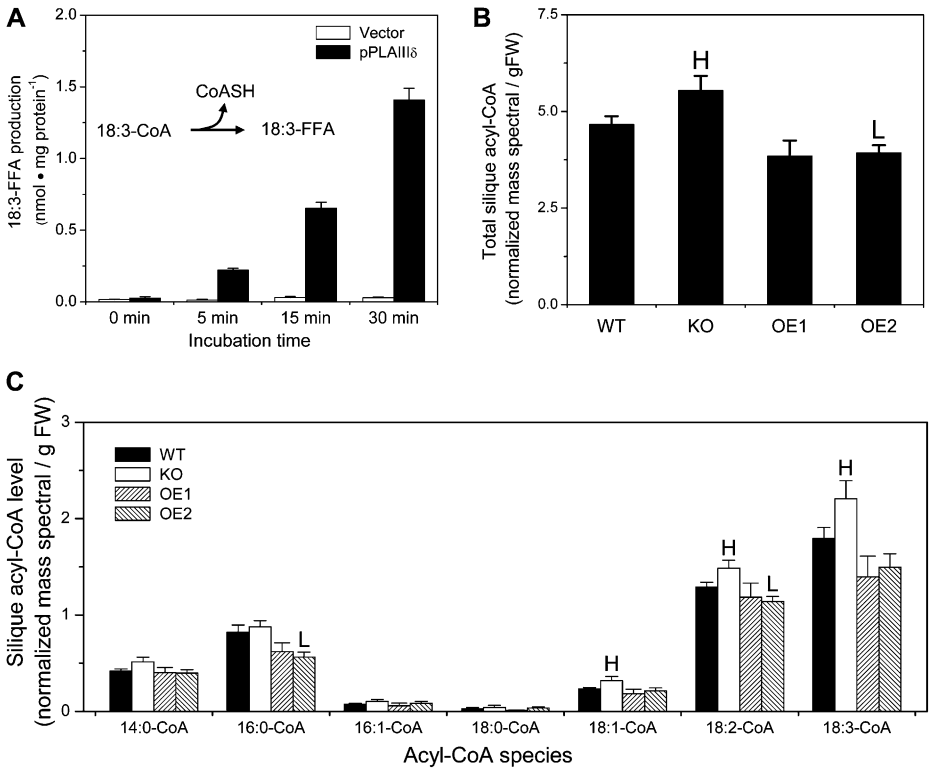


**Figure 6.** pPLAIIIδ hydrolyzes acyl-CoA and affects acyl-CoA levels in Arabidopsis. A, FFA 18:3 (18:3-FFA) released from 18:3-CoA in 16:0-18:2 PC vesicles by purified pPLAIIIδ. Vector refers to a control in which proteins from *E. coli* transformed with an empty vector were isolated using the same immunoaffinity procedure for purifying pPLAIIIδ-6×His. Values are means ± SE ($n = 3$). B, Total acyl-CoA contents in developing Arabidopsis siliques of wild-type (WT), *pPLAIIIδ* KO, OE, and COM plants. FW, Fresh weight. C, Levels of acyl-CoA molecular species in developing siliques of wild-type, *pPLAIIIδ* KO, OE, and COM plants. Acyl-CoAs were extracted from developing siliques 7 d post pollination and analyzed by liquid chromatography-ESI-MS/MS. Values are means ± SE ($n = 5$). $^{H}$Significantly higher and $^{L}$significantly lower, each at $P < 0.05$ compared with the wild type, based on Student's *t* test.

### pPLAIIIδ Is Associated with the Plasma and Intracellular Membranes

To determine its subcellular association, a GFP-tagged pPLAIIIδ was expressed in Arabidopsis, and the green fluorescence signal of pPLAIIIδ-GFP was mostly detected on the inner cell boundary of leaf epidermal cells (Fig. 7A). Plasmolysis by applying saline solution to the roots showed that the GFP signal in root epidermal cells was shrinking along with the plasma membrane (Fig. 7B). To further analyze the intracellular association, total leaf proteins were fractionated into cytosolic and microsomal fractions. All pPLAIIIδ-GFP was associated with the microsomal membranes but not with cytosol (Fig. 7C). The microsomal proteins were further partitioned into the plasma membrane and intracellular membrane fractions. Approximately 80% of pPLAIIIδ-GFP was associated with the plasma membrane, whereas 20% was associated with intracellular membranes based on the intensity of the protein bands (Fig. 7C). These data indicate that pPLAIIIδ is associated with both the plasma and intracellular membranes.

### Seed-Specific OE of *pPLAIIIδ* Increases Oil Content

The increased oil content in seeds raises the question of whether increased pPLAIIIδ expression can be used to increase seed oil production. However, constitutive OE of *pPLAIIIδ* resulted in a decrease in plant height and overall seed yield (Fig. 8, A and B). The seed yield per *35S::pPLAIIIδ-OE* plants was approximately 50% of that of wild-type plants (Fig. 8B). To explore whether the improved oil content could be uncoupled from decreased seed production, we placed *pPLAIIIδ* under the control of the seed-specific promoter of soybean (*Glycine max*) *β-conglycinin* (*CON::pPLAIIIδ*; Supplemental Fig. S4A). The level of pPLAIIIδ expression in developing siliques was 25-fold higher in *CON::pPLAIIIδ* than that in the wild type (Fig. 8C). The presence of the pPLAIIIδ-GFP protein was detectable by visualizing the GFP fluorescence (Supplemental Fig. S4B). *CON::pPLAIIIδ* plant height and seed yield were comparable with the wild type (Fig. 8, A and B). In three *CON::pPLAIIIδ* lines tested, seed oil content was increased over wild-type seeds (39% versus 35%; Fig. 8D). While oil content per *CON::pPLAIIIδ* seed weight was lower than that per *35S::pPLAIIIδ* seed weight (Figs. 1D and 8D), the overall seed oil production per *CON::pPLAIIIδ* plant was significantly higher than that per *35S::pPLAIIIδ*, due to the higher seed yield per plant (Fig. 8B), and per wild-type plant, due to the increased oil content without change in seed yield (Fig. 8, B and D).

The seed-specific overexpression of *pPLAIIIδ* resulted in changes in fatty acid composition, and the changes in *CON::pPLAIIIδ* were similar to those in *35S::pPLAIIIδ* seeds. The percentages of 18:1 and 18:2 were lower, while those of 20:0, 20:1, 20:1, and 22:1 were higher, in *CON::pPLAIIIδ* lines than in the wild type (Fig. 8E). The ratio of 20:1 to 18:1 was 30% higher in *CON::pPLAIIIδ* lines than in the wild type (Supplemental Fig. S4C), and the same pattern was observed when total 20-carbon fatty acids were compared

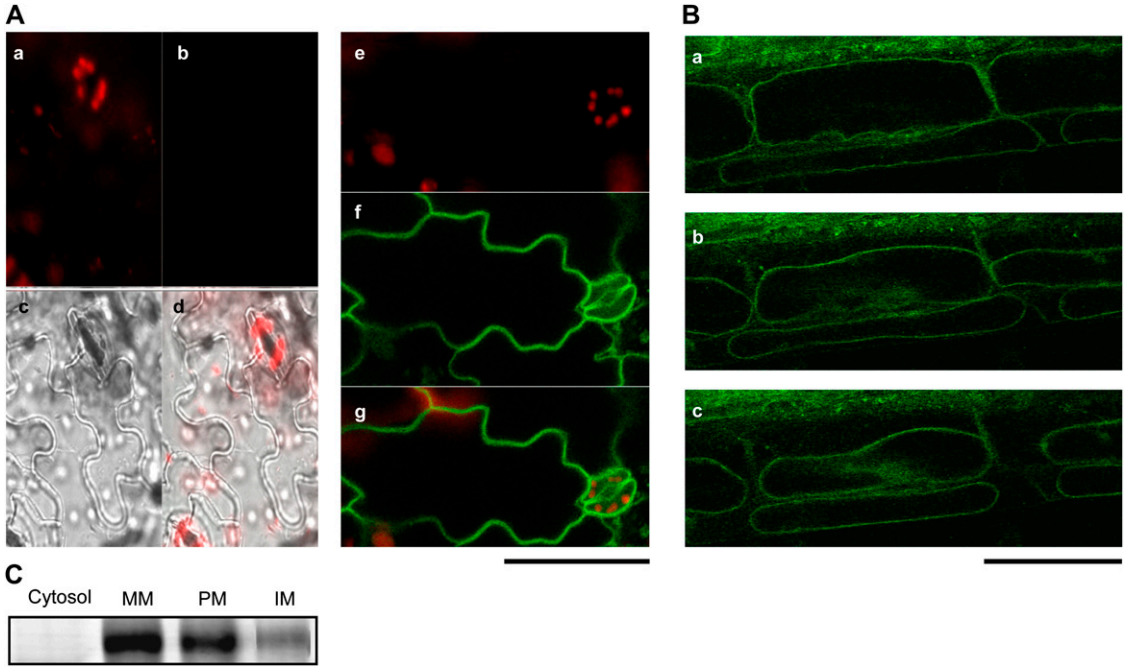


**Figure 7.** Subcellular localization of pPLAIIIδ in Arabidopsis. A, Confocal imaging of epidermal cells of wild-type leaf (a–d) and *pPLAIIIδ-OE*:GFP leaf (e–g) chlorophyll fluorescence (a and e; red) versus GFP (b and f; green). The green fluorescent signal of the GFP-tagged pPLAIIIδ protein is shown in f. Transmitted light (c) and overlay (d) clarify cell outlines. Bar = 50 μm. B, Plasmolysis of root epidermal cells of the pPLAIIIδ-OE:GFP mutant: a, at 1 min after plasmolysis, the green fluorescence signal was located close to the cell wall; b and c, at 3 and 5 min after plasmolysis, respectively, the green fluorescence signal was colocalized with plasma membrane during cell shrink. Bar = 50 μm. C, Immunoblotting of pPLAIIIδ-GFP using GFP antibodies in subcellular fractions. Soluble protein (20 μg per lane) and membrane protein (5 μg per lane) were used in SDS-PAGE, followed by immunoblotting. Cytosol, Soluble fraction; MM, microsomal membrane fraction; PM, plasma membrane; IM, intracellular membrane.

with total 18-carbon fatty acids (Supplemental Fig. S4D). These results indicate that pPLAIIIδ affects TAG metabolism in the same manner regardless of the promoter used and that the use of seed-specific expression of *pPLAIIIδ* has the potential to be applied for increased seed oil production.

## DISCUSSION

These data show that pPLAIIIδ positively impacts seed oil content. Whereas pPLAIIIδ-KO decreases seed oil content, pPLAIIIδ-OE, driven either by a constitutive or a seed-specific promoter, increases seed oil content. pPLAIIIδ hydrolyzes PC to generate FFA and LPC. pPLAIIIδ may accelerate acyl flux from the plastid to the ER and, therefore, enhance glycerolipid synthesis. Fatty acids in higher plants are synthesized exclusively in the plastid and have to be exported to the ER, where glycerolipids are synthesized (Fig. 9). Lipid trafficking between organelles is a fundamental, yet poorly understood, process in plants. In recent years, excellent progress has been made toward understanding lipid transport from the ER to the plastid for the synthesis of galactolipids (Wang et al., 2012b). Phosphatidic acid (PA) is imported into the plastid through a protein complex (Wang and Benning, 2012). In contrast, the metabolic and regulatory mechanisms by which fatty acids in the plastid are trafficked to the ER are unknown.

16:0 and 18:1 are two major fatty acids exported from the plastid in Arabidopsis (Pidkowich et al., 2007; Li-Beisson et al., 2010). FFAs are thought to be able to cross membrane bilayers through diffusion and possibly protein-mediated translocation (Wang and Benning, 2012). After reaching the plastid outer envelope, long-chain acyl-CoA synthetases convert these fatty acids to acyl-CoA. In the conventional Kennedy pathway, acyl-CoA is used for the sequential acylation of glycerol-3-P → LPA → PA → DAG → TAG (Fig. 9). However, kinetic labeling data indicate that fatty acids exported from the plastid are first incorporated into PC and then channeled to TAG in soybean embryos (Bates et al., 2009, 2012; Bates and Browse, 2011). The presence of highly active LPCAT on the Arabidopsis plastid outer envelope membrane is consistent with the formation of PC using fatty acids from the plastids (Tjellström et al., 2012; Wang et al., 2012a). Recent data indicate that LPCAT1 and LPCAT2 catalyze the incorporation of fatty acids into PC in Arabidopsis seeds (Bates et al., 2012; Wang et al., 2012a). However, knowledge is lacking about

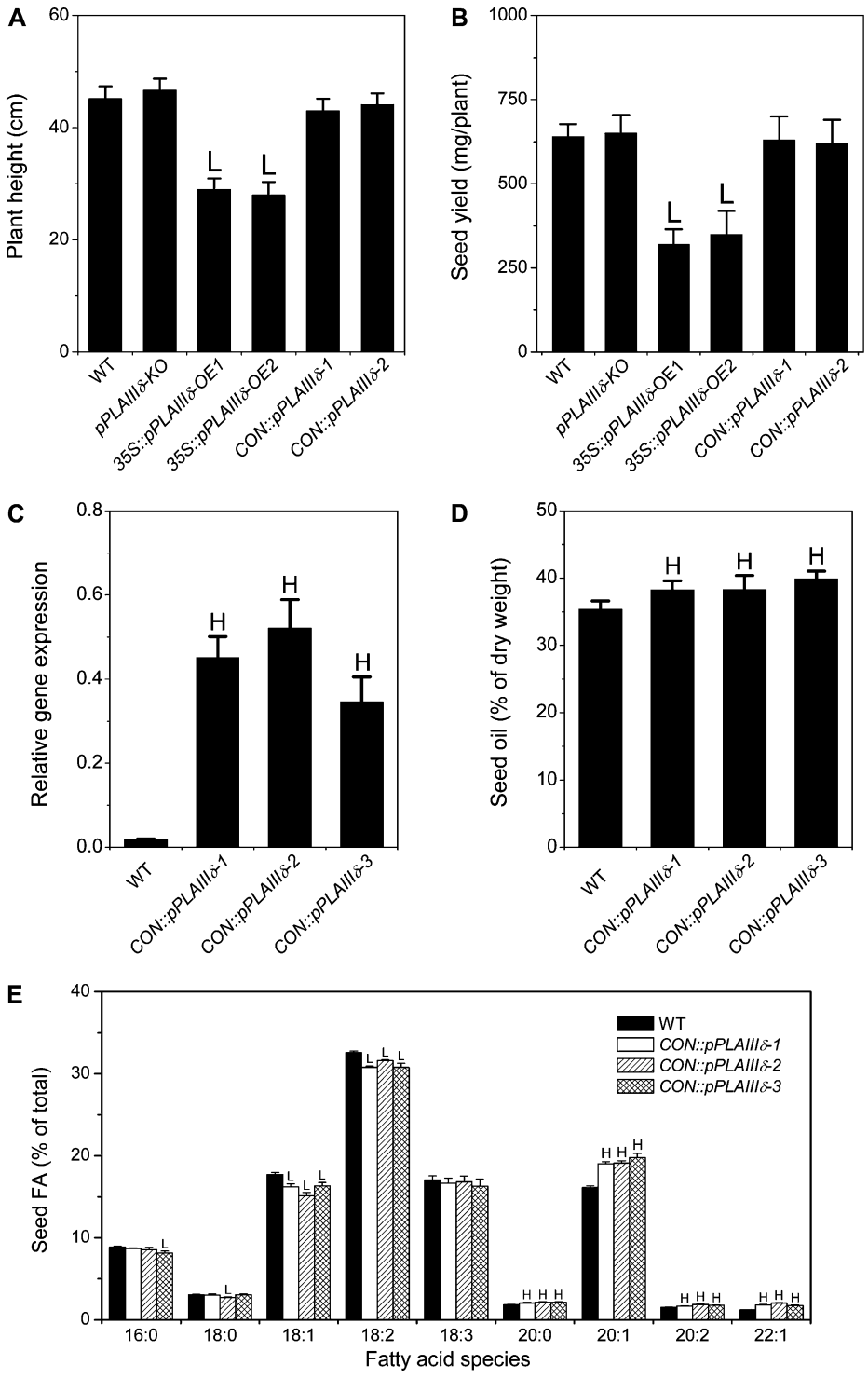


**Figure 8.** Seed-specific OE of *pPLAIIIδ* increases oil content without compromising seed production. A, Plant heights of mature wild-type (WT), *pPLAIIIδ-KO*, *35S::pPLAIIIδ*, and *CON::pPLAIIIδ* plants. 35S represents the cauliflower mosaic virus 35S promoter, and CON represents the promoter of soybean β-conglycinin. Values are means ± SE ($n = 5$). B, Seed yield per plant of wild-type, *pPLAIIIδ-KO*, *35S::pPLAIIIδ*, and *CON::pPLAIIIδ* plants. Values are means ± SE ($n = 5$). C, Transcript levels of *pPLAIIIδ* in developing siliques of the wild type and three independent *CON::pPLAIIIδ* lines. The RNA level was determined by real-time PCR and normalized in comparison with *UBQ10*. Values are means ± SE ($n = 3$). D, Seed oil contents in the wild type and three independent *CON::pPLAIIIδ* lines. Values are means ± SE ($n = 3$). E, Fatty acid (FA) composition in wild-type and *CON::pPLAIIIδ* seeds. Values are means ± SE ($n = 3$). $^{H}$Significantly higher and $^{L}$significantly lower, each at $P < 0.05$ compared with the wild type, based on Student's *t* test.

what enzyme produces LPC that impacts TAG synthesis. PDAT can transfer a fatty acid from PC to DAG to produce TAG and LPC, but its role in TAG production in seeds remains unclear (Chapman and Ohlrogge, 2012). pPLAIIIδ could be one of the enzymes hydrolyzing PC to produce an FFA and LPC that LPCAT uses to accept fatty acids from the plastid (Fig. 9). The combined activity of pPLAIII and LPCATs may modulate the rate of fatty acid trafficking from the plastid to the ER in Arabidopsis seeds.

Fatty acids, such as 18:1, released from PC by pPLAIIIδ may enter the acyl-CoA pool for elongation (Fig. 9). KO and OE of the pPLAIIIδ gene displayed opposite effects on the levels of 18:1 and 20:1 fatty acids in seed oil. Detailed profiling of TAG molecules

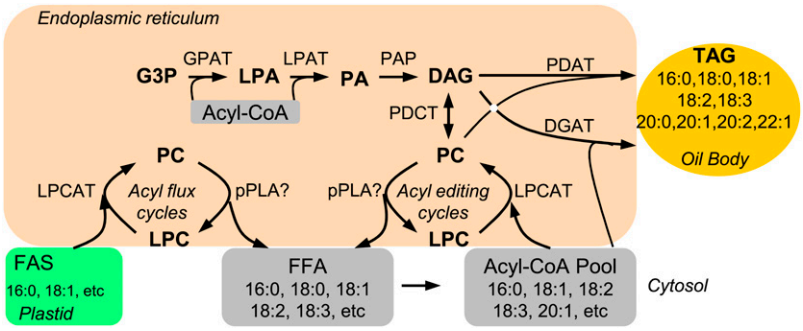


**Figure 9.** Potential function of pPLAIIIδ in fatty acyl flux from plastid to the ER and fatty acyl editing in the ER. Fatty acids are exclusively synthesized in plastids, whereas glycerolipids are assembled in the ER. In Arabidopsis, the fatty acids exported from plastids are primarily 16:0 and 18:1, but seed TAGs are enriched in 18:2, 18:3, and 20:1. Therefore, fatty acyl flux and fatty acyl editing are needed in seed oil accumulation. pPLA may hydrolyze PC to generate LPC and FFA, where LPC can be reused by LPCAT to form PC and FFA can be esterified to form acyl-CoA. pPLA may also hydrolyze acyl-CoA to FFA. PC and acyl-CoA are the sites for fatty acyl editing, such as desaturation and elongation. PAP, PA phosphatase. [See online article for color version of this figure.]

also showed the opposite effects on the levels of 18:1-containing and 20:1-containing TAGs by KO and OE of the pPLAIIIδ gene. In Arabidopsis, the major fatty acids exported from plastids to the ER are 16:0, 18:0, and 18:1. In the ER, 18:1 on PC is desaturated to 18:2 and 18:3 (Li-Beisson et al., 2010), whereas acyl-CoA is used for fatty acid elongation to form longer chain fatty acids, such as 20:1 (Joubès et al., 2008; Li-Beisson et al., 2010). The effect of pPLAIIIδ on fatty acid composition is distinctively different from that of the recently described PC:DAG cholinephosphotransferase that transfers phosphocholine from PC to DAG, and a mutation of PC:DAG cholinephosphotransferase decreases the 18:2 and 18:3 level in Arabidopsis seed TAG by 40% (Lu et al., 2009). Thus, the increased pPLAIIIδ expression may facilitate the release of 18:1 from PC for 20:1 production (Fig. 9).

Compared with the wild type, OE of pPLAIIIδ had a lower acyl-CoA pool size in developing silique and higher seed oil content. The decrease in the acyl-CoA pool size could result from the thioesterase activity of pPLAIIIδ and/or increased PC turnover and TAG synthesis. The exchange of modified acyl groups between PC and the acyl-CoA pool requires extensive acyl editing cycles (Harwood, 1996). Through the acyl editing cycles, modified fatty acids enter the acyl-CoA pool to be utilized for glycerolipid synthesis, and acyl-CoA can be channeled into PC for further modification and directly for TAG production (Stymne and Stobart, 1984; Bafor et al., 1991; Bates et al., 2007, 2009). The inverse association between acyl-CoA pool and TAG contents could mean that the pPLAIIIδ-catalyzed turnover of acyl-CoA and PC promotes seed oil accumulation.

The enhanced mRNA level of genes, such as AAPT and CCT, in PC biosynthesis in *pPLAIIIδ-OE* plants indicates that increased pPLAIIIδ-mediated PC hydrolysis leads to an increase in PC biosynthesis and, thus, increased PC turnover. Meanwhile, RNA levels are higher for genes in the Kennedy pathway, such as GPAT, LPAT, PA phosphatase, and DGAT, in developing *pPLAIIIδ-OE* siliques. The increased transcript levels of glycerolipid-producing genes may be a feed-forward stimulation by enhanced substrate supplies, as the increased *pPLAIIIδ* expression leads to elevated levels of FFAs and LPC. How the metabolic changes in FFAs and LPC are connected to the altered mRNA levels and potentially gene expression requires further investigation. In budding yeast (*Saccharomyces cerevisiae*), it has been shown that the transcriptional factor directly binds to PA, senses cellular PA levels, and regulates the expression of many genes involved in membrane lipid synthesis (Loewen et al., 2004). In addition, there is an increase in the mRNA level of LPCAT, which catalyzes the acylation of LPC using fatty acids from the plastid. This could mean an increase in fatty acid trafficking from the plastid to the ER, where glycerolipids are synthesized. Further studies are needed to determine the mechanism by which increased *pPLAIIIδ* expression promotes TAG production. Such investigation of how a lipid-hydrolyzing enzyme, such as pPLAIIIδ, promotes lipid accumulation has the potential to better our understanding of lipid metabolism and accumulation.

In summary, our study shows that pPLAIIIδ hydrolyzes PC to generate FFA and LPC and that genetic alterations of *pPLAIIIδ* expression change seed oil content and fatty acid composition in Arabidopsis seeds. Our large-scale TAG species analysis reveals that pPLAIIIδ promotes the production of 20:1-TAG. We propose that pPLAIIIδ plays a role in fatty acyl flux from the plastid to the ER and/or PC fatty acyl remodeling for TAG synthesis. Furthermore, these results indicate that the use of seed-specific expression of *pPLAIIIδ* has the potential to improve seed oil production in crops.

## MATERIALS AND METHODS

### Generation of *pPLAIII* KO, OE, and Complementation Plants

Arabidopsis (*Arabidopsis thaliana*) T-DNA insertional mutants for *pPLAIIIα* (Salk_040363), *pPLAIIIβ* (Salk_057212), *pPLAIIIγ* (Salk_088404), and *pPLAIIIδ* (Salk_029470) were identified from the Salk Arabidopsis T-DNA KO collection obtained from the Arabidopsis Biological Resource Center. The homozygous T-DNA insertion mutant for individual *pPLAIIIs* was verified by PCR-based screening using a T-DNA left border primer and gene-specific primers as listed in Supplemental Table S1. The isolation of *pPLAIIIβ-KO* was reported previously (Li et al., 2011). The loss of gene transcripts in *pPLAIII-KO* was confirmed by real-time PCR. To generate the complementation lines (*pPLAIIIδ-COM*), the genomic DNA sequence of *pPLAIIIδ* from the promoter region to the terminator region was cloned using two primers as listed in Supplemental Table S1 and fused into binary vector pEC291 for plant transformation.

To overexpress pPLAIIIδ, the genomic sequence of *pPLAIIIδ* was obtained by PCR using ecotype Columbia Arabidopsis genomic DNA as a template and primers listed in Supplemental Table S1. The genomic DNA was cloned into the pMDC83 vector before the GFP-His coding sequence. The expression of *pPLAIIIδ* was under the control of the 35S cauliflower mosaic virus promoter or the promoter of soybean (*Glycine max*) β-conglycinin. The sequences of the fusion constructs were verified by sequencing before they were introduced into the *Agrobacterium tumefaciens* strain C58C1. Ecotype Columbia Arabidopsis plants were transformed, and transgenic plants were screened and confirmed by antibiotic selection and PCR. Over 15 independent transgenic lines were obtained (*pPLAIIIδ-OE*) with similar plant stature. Five independent lines of *pPLAIIIδ-OE* were further verified by immunoblotting with anti-GFP antibody.

### RNA Extraction and Real-Time PCR

Real-time PCR was performed as described previously (Li et al., 2006, 2011). Briefly, total RNA was extracted from different tissues using the cetyltrimethylammonium bromide method (Stewart and Via, 1993). DNA contamination in RNA samples was removed with RNase-free DNase. An iScript kit (Bio-Rad) was used to synthesize complementary DNA (cDNA) from isolated RNA template by reverse transcription. The MyiQ sequence detection system (Bio-Rad) was used to detect products during quantitative real-time PCR by monitoring SYBR Green fluorescent labeling of double-stranded DNA. Efficiency was normalized to a control gene, *UBQ10*. The real-time PCR primers are listed in Supplemental Table S2. The data were expressed as means ± SE ($n = 3$ replicates). PCR conditions were as follows: one cycle of 95°C for 1 min; 40 cycles of DNA melting at 95°C for 30 s, DNA annealing at 55°C for 30 s, and DNA extension at 72°C for 30 s; and final extension of DNA at 72°C for 10 min.

### Analysis of Fatty Acid Composition and Oil Content

Ten milligrams of Arabidopsis seeds was placed in glass tubes with Teflon-lined screw caps, and 1.5 mL of 5% (v/v) $H_2SO_4$ in methanol with 0.2% butylated hydroxytoluene was added. The samples were incubated for 1 h at 90°C for oil extraction and transmethylation. Fatty acid methyl esters (FAMEs) were extracted with hexane. FAMEs were quantified using gas chromatography on a SUPELCOWAX-10 (0.25 mm × 30 m) column with helium as a carrier gas at 20 mL $min^{-1}$ and detection by flame ionization. The oven temperature was maintained at 170°C for 1 min and then ramped to 210°C at 3°C $min^{-1}$. FAMEs from TAG were identified by comparing their retention times with FAMEs in a standard mixture. Heptadecanoic acid (17:0) was used as the internal standard to quantify the amounts of individual fatty acids. Fatty acid composition is expressed in weight percentage.

### *pPLAIIIδ* Cloning and Protein Purification from *Escherichia coli*

The full-length cDNA of *pPLAIIIδ* was obtained by PCR using an Arabidopsis cDNA library as a template and a pair of primers as listed in Supplemental Table S1. The cDNA was cloned into the pET28a vector before the 6×His coding sequence. The 6×His fusion construct was sequenced and confirmed to be error free before it was introduced into *E. coli* strain Rosetta (DE3; Amersham Biosciences). The bacteria were grown to an optical density at 600 nm of 0.7 and induced with 0.1 mM isopropyl 1-thio-β-D-galactopyranoside for 16 h at 16°C. The pPLAIIIδ-6×His fusion protein was purified as described previously (Pappan et al., 2004). Briefly, the bacterial pellet was resuspended in STE buffer containing 1 mg $mL^{-1}$ lysozyme (50 mM Tris-HCl, pH 8.0, 150 mM NaCl, and 1 mM EDTA). The samples were kept on ice for 30 min. Dithiothreitol and *N*-laurylsarcosine (Sarkosyl) were added to a final concentration of 5 mM and 1.5% (w/v), respectively. The suspension was vortexed and sonicated on ice for 5 min. After centrifugation at 10,000*g* for 20 min, the supernatant was transferred to a new tube. Triton X-100 was added to a final concentration of 4% (v/v), and 6×His agarose beads were added (10%, w/v). The solution was gently rotated at 25°C for 1 h. The fusion proteins bound to agarose beads were washed with 20 volumes of STE buffer. The amount of purified protein was measured with a protein assay kit (Bio-Rad).

### Enzyme Assays

Phospholipids and acyl-CoAs were purchased from Avanti Polar Lipids. PC or 18:3-CoA in chloroform was dried under a nitrogen stream and emulsified in reaction buffer (25 mM HEPES, pH 7.5, 10 mM $CaCl_2$, and 10 mM $MgCl_2$) by vortexing, followed by 5 min of sonication on ice. Acyl-hydrolyzing activities were assayed in a reaction mixture containing 25 mM HEPES, pH 7.5, 10 mM $CaCl_2$, 10 mM $MgCl_2$, and 60 μmol PC as substrate. Ten micrograms of purified protein was added to the mixture in a final volume of 500 μL. The reaction was incubated at 30°C for the indicated times and stopped by adding 2 mL of chloroform:methanol (2:1, v/v) and 500 μL of 25 mM LiCl. After vortexing and separation by centrifugation, the lower phase was transferred to a new glass tube. The upper phase was extracted twice more by adding 1 mL of chloroform each time, and the three lower phases were combined. Lipid internal standards were added, and lipid quantification was performed by mass spectrometry as described below.

### Lipid Quantification

In in vitro enzyme assays, lipids were extracted for analysis as described previously (Li et al., 2011). Twenty microliters of lipid sample was combined with 340 μL of chloroform and 840 μL of chloroform:methanol:300 mM ammonium acetate in water (300:665:35). FFAs were determined by ESI-MS on an electrospray ionization triple quadruple mass spectrometer (API4000; Applied Biosystems), using the deuterated internal standard (7,7,8,8-d4-16:0 fatty acid; Sigma-Aldrich), by scanning in negative ion mode from mass-to-charge ratio 200 to 350 (Li et al., 2011). LPC was determined with the same instrument as described previously (Li et al., 2011). Plants for acyl-CoA measurement were grown in growth chambers with a 12-h-light/12-h-dark cycle, at 23°C/21°C, 50% humidity, and 200 μmol $m^{-2}$ $s^{-1}$ light intensity, and watered with fertilizer once per week. Acyl-CoAs were extracted and analyzed by liquid chromatography-ESI-MS/MS as described previously (Magnes et al., 2005; Han et al., 2010). TAG molecular species were analyzed by ESI-MS/MS using neutral loss scan modes (Lee et al., 2011, 2012). The TAG analysis is described in detail in Supplemental Materials and Methods S1.

### Microscopy Imaging and Subcellular Fractionation

The subcellular location of GFP-tagged protein was determined using a Zeiss LSM 510 confocal microscope equipped with a ×40 differential interference contrast, 1.2-numerical aperture water-immersion lens, with excitation using the 488-nm line of an argon gas laser and a 500- to 550-nm band-pass emission filter. Plasmolysis in primary root cells was induced by immersing roots in 0.5 M NaCl for 1, 3, and 5 min. Developing seeds from Arabidopsis siliques were imaged using a Nikon Eclipse 800 wide-field microscope and a ×60 differential interference contrast, 1.2-numerical aperture objective, with mercury lamp excitation and a 492/18 band pass excitation filter and a 535/40 band emission filter. For subcellular fractionation, proteins were extracted from leaves of 4-week-old plants using buffer (30 mM HEPES, pH 7.5, 400 mM NaCl, and 1 mM phenylmethanesulfonyl fluoride), followed by centrifugation at 6,000*g* for 10 min. The supernatant was centrifuged at 100,000*g* for 60 min. The resulting supernatant is referred to as the soluble cytosol fraction, and the pellet is referred to as the microsomal fraction. The microsomal fraction was separated further into the plasma and intracellular membrane fractions, using two-phase partitioning as described previously (Fan et al., 1999).

## SDS-PAGE and Immunoblotting

Leaf samples, each weighing approximately 1 g, were harvested and ground in 3 mL of buffer of 30 mM HEPES, pH 7.5, 400 mM NaCl, 1.0 mM phenylmethanesulfonyl fluoride, and 1 mM dithiothreitol. Proteins were separated by 8% SDS-PAGE and transferred to a polyvinylidene difluoride membrane. The membrane was visualized with alkaline phosphatase conjugated to a secondary anti-mouse antibody after blotting with GFP antibody.

Sequence data from this article can be found in the Arabidopsis Genome Initiative database under the following accession numbers: *AAPT1*, At1g13560; *AAPT2*, At3g25585; *CCT1*, At2g32260; *CCT2*, At4g15130; *DGAT1*, At2g19450; *DGAT2*, At3g51520; *GPAT*, At1g32200; *LPAT2*, At3g57650; *LPAT3*, At1g51260; *LPAT4*, At1g75020; *LPAT5*, At3g18850; *LPCAT1*, At1g63050; *PAH1*, At3g09560; *PDAT1*, At5g13640; *pPLAI*, At1g61850; *pPLAIIα*, At2g26560; *pPLAIIβ*, At4g37050; *pPLAIIγ*, At4g37070; *pPLAIIδ*, At4g37060; *pPLAIIε*, At5g43590; *pPLAIIIα*, At2g39220; *pPLAIIIβ*, At3g54950; *pPLAIIIγ*, At4g29800; *pPLAIIIδ*, At3g63200; and *UBQ10*, At4g05320.

## Supplemental Data

The following materials are available in the online version of this article.

**Supplemental Figure S1.** Generation of KO, OE, and complementation mutants of *pPLAIIIs*.

**Supplemental Figure S2.** RNA accumulation patterns of four pPLAIII genes in developing Arabidopsis seeds.

**Supplemental Figure S3.** pPLAIIIδ promotes increased levels of 20C fatty acyl-containing TAG over 18C fatty acyl-containing TAG in Arabidopsis seeds, as determined by mass spectral analysis.

**Supplemental Figure S4.** Seed-specific OE of *pPLAIIIδ* in Arabidopsis.

**Supplemental Table S1.** PCR primers for mutant screening and molecular cloning.

**Supplemental Table S2.** Real-time PCR primers for quantitative measurement of transcript levels.

**Supplemental Materials and Methods S1.** Mass spectral analysis of TAG.

## ACKNOWLEDGMENTS

We thank Howard Berg at the Donald Danforth Plant Science Center's Integrated Microscopy Facility for imaging assistance.

Received February 27, 2013; accepted March 27, 2013; published March 29, 2013.

## LITERATURE CITED

**Bafor M, Smith MA, Jonsson L, Stobart K, Stymne S** (1991) Ricinoleic acid biosynthesis and triacylglycerol assembly in microsomal preparations from developing castor-bean (*Ricinus communis*) endosperm. Biochem J **280:** 507–514

**Bates PD, Browse J** (2011) The pathway of triacylglycerol synthesis through phosphatidylcholine in Arabidopsis produces a bottleneck for the accumulation of unusual fatty acids in transgenic seeds. Plant J **68:** 387–399

**Bates PD, Browse J** (2012) The significance of different diacylgycerol synthesis pathways on plant oil composition and bioengineering. Front Plant Sci **3:** 147

**Bates PD, Durrett TP, Ohlrogge JB, Pollard M** (2009) Analysis of acyl fluxes through multiple pathways of triacylglycerol synthesis in developing soybean embryos. Plant Physiol **150:** 55–72

**Bates PD, Fatihi A, Snapp AR, Carlsson AS, Browse J, Lu C** (2012) Acyl editing and headgroup exchange are the major mechanisms that direct polyunsaturated fatty acid flux into triacylglycerols. Plant Physiol **160:** 1530–1539

**Bates PD, Ohlrogge JB, Pollard M** (2007) Incorporation of newly synthesized fatty acids into cytosolic glycerolipids in pea leaves occurs via acyl editing. J Biol Chem **282:** 31206–31216

**Bourgis F, Kilaru A, Cao X, Ngando-Ebongue GF, Drira N, Ohlrogge JB, Arondel V** (2011) Comparative transcriptome and metabolite analysis of oil palm and date palm mesocarp that differ dramatically in carbon partitioning. Proc Natl Acad Sci USA **108:** 12527–12532

**Chapman KD, Ohlrogge JB** (2012) Compartmentation of triacylglycerol accumulation in plants. J Biol Chem **287:** 2288–2294

**Dyer JM, Stymne S, Green AG, Carlsson AS** (2008) High-value oils from plants. Plant J **54:** 640–655

**Fan L, Zheng S, Cui D, Wang X** (1999) Subcellular distribution and tissue expression of phospholipase Dα, Dβ, and Dγ in Arabidopsis. Plant Physiol **119:** 1371–1378

**Han J, Clement JM, Li J, King A, Ng S, Jaworski JG** (2010) The cytochrome P450 CYP86A22 is a fatty acyl-CoA omega-hydroxylase essential for estolide synthesis in the stigma of Petunia hybrida. J Biol Chem **285:** 3986–3996

**Harwood JL** (1996) Recent advances in the biosynthesis of plant fatty acids. Biochim Biophys Acta **1301:** 7–56

**Hayden DM, Rolletschek H, Borisjuk L, Corwin J, Kliebenstein DJ, Grimberg A, Stymne S, Dehesh K** (2011) Cofactome analyses reveal enhanced flux of carbon into oil for potential biofuel production. Plant J **67:** 1018–1028

**Huang S, Cerny RE, Bhat DS, Brown SM** (2001) Cloning of an Arabidopsis patatin-like gene, *STURDY*, by activation T-DNA tagging. Plant Physiol **125:** 573–584

**Joubès J, Raffaele S, Bourdenx B, Garcia C, Laroche-Traineau J, Moreau P, Domergue F, Lessire R** (2008) The VLCFA elongase gene family in Arabidopsis thaliana: phylogenetic analysis, 3D modelling and expression profiling. Plant Mol Biol **67:** 547–566

**La Camera S, Geoffroy P, Samaha H, Ndiaye A, Rahim G, Legrand M, Heitz T** (2005) A pathogen-inducible patatin-like lipid acyl hydrolase facilitates fungal and bacterial host colonization in Arabidopsis. Plant J **44:** 810–825

**Lee J, Welti R, Roth M, Schapaugh WT, Li J, Trick HN** (2012) Enhanced seed viability and lipid compositional changes during natural ageing by suppressing phospholipase Dα in soybean seed. Plant Biotechnol J **10:** 164–173

**Lee J, Welti R, Schapaugh WT, Trick HN** (2011) Phospholipid and triacylglycerol profiles modified by *PLD* suppression in soybean seed. Plant Biotechnol J **9:** 359–372

**Li M, Bahn SC, Guo L, Musgrave W, Berg H, Welti R, Wang X** (2011) Patatin-related phospholipase pPLAIIIβ-induced changes in lipid metabolism alter cellulose content and cell elongation in *Arabidopsis*. Plant Cell **23:** 1107–1123

**Li M, Qin C, Welti R, Wang X** (2006) Double knockouts of phospholipases Dζ1 and Dζ2 in Arabidopsis affect root elongation during phosphate-limited growth but do not affect root hair patterning. Plant Physiol **140:** 761–770

**Li-Beisson Y, Shorrosh B, Beisson F, Andersson MX, Arondel V, Bates PD, Baud S, Bird D, Debono A, Durrett TP, et al** (2010) Acyl-lipid metabolism. The Arabidopsis Book **8:** e0133,

**Loewen CJ, Gaspar ML, Jesch SA, Delon C, Ktistakis NT, Henry SA, Levine TP** (2004) Phospholipid metabolism regulated by a transcription factor sensing phosphatidic acid. Science **304:** 1644–1647

**Lu C, Xin Z, Ren Z, Miquel M, Browse J** (2009) An enzyme regulating triacylglycerol composition is encoded by the ROD1 gene of Arabidopsis. Proc Natl Acad Sci USA **106:** 18837–18842

**Magnes C, Sinner FM, Regittnig W, Pieber TR** (2005) LC/MS/MS method for quantitative determination of long-chain fatty acyl-CoAs. Anal Chem **77:** 2889–2894

**Murakami M, Taketomi Y, Miki Y, Sato H, Hirabayashi T, Yamamoto K** (2011) Recent progress in phospholipase $A_2$ research: from cells to animals to humans. Prog Lipid Res **50:** 152–192

**Pappan K, Zheng L, Krishnamoorthi R, Wang X** (2004) Evidence for and characterization of $Ca^{2+}$ binding to the catalytic region of Arabidopsis thaliana phospholipase Dbeta. J Biol Chem **279:** 47833–47839

**Pidkowich MS, Nguyen HT, Heilmann I, Ischebeck T, Shanklin J** (2007) Modulating seed beta-ketoacyl-acyl carrier protein synthase II level converts the composition of a temperate seed oil to that of a palm-like tropical oil. Proc Natl Acad Sci USA **104:** 4742–4747

**Rietz S, Dermendjiev G, Oppermann E, Tafesse FG, Effendi Y, Holk A, Parker JE, Teige M, Scherer GF** (2010) Roles of Arabidopsis patatin-related phospholipases a in root development are related to auxin responses and phosphate deficiency. Mol Plant **3:** 524–538

**Rietz S, Holk A, Scherer GF** (2004) Expression of the patatin-related phospholipase A gene AtPLA IIA in Arabidopsis thaliana is up-regulated by salicylic acid, wounding, ethylene, and iron and phosphate deficiency. Planta **219:** 743–753

**Rogalski M, Carrer H** (2011) Engineering plastid fatty acid biosynthesis to improve food quality and biofuel production in higher plants. Plant Biotechnol J **9:** 554–564

**Scherer GF, Ryu SB, Wang X, Matos AR, Heitz T** (2010) Patatin-related phospholipase A: nomenclature, subfamilies and functions in plants. Trends Plant Sci **15:** 693–700

**Stewart CN Jr, Via LE** (1993) A rapid CTAB DNA isolation technique useful for RAPD fingerprinting and other PCR applications. Biotechniques **14:** 748–750

**Stymne S, Stobart AK** (1984) Evidence for the reversibility of the acyl-CoA: lysophosphatidylcholine acyltransferase in microsomal preparations from developing safflower (*Carthamus tinctorius* L.) cotyledons and rat liver. Biochem J **223:** 305–314

**Tjellström H, Yang Z, Allen DK, Ohlrogge JB** (2012) Rapid kinetic labeling of Arabidopsis cell suspension cultures: implications for models of lipid export from plastids. Plant Physiol **158:** 601–611

**Wang L, Shen W, Kazachkov M, Chen G, Chen Q, Carlsson AS, Stymne S, Weselake RJ, Zou J** (2012a) Metabolic interactions between the Lands cycle and the Kennedy pathway of glycerolipid synthesis in *Arabidopsis* developing seeds. Plant Cell **24:** 4652–4669

**Wang Z, Benning C** (2012) Chloroplast lipid synthesis and lipid trafficking through ER-plastid membrane contact sites. Biochem Soc Trans **40:** 457–463

**Wang Z, Xu C, Benning C** (2012b) TGD4 involved in endoplasmic reticulum-to-chloroplast lipid trafficking is a phosphatidic acid binding protein. Plant J **70:** 614–623

**Weselake RJ, Taylor DC, Rahman MH, Shah S, Laroche A, McVetty PB, Harwood JL** (2009) Increasing the flow of carbon into seed oil. Biotechnol Adv **27:** 866–878

**Yang W, Devaiah SP, Pan X, Isaac G, Welti R, Wang X** (2007) AtPLAI is an acyl hydrolase involved in basal jasmonic acid production and Arabidopsis resistance to *Botrytis cinerea*. J Biol Chem **282:** 18116–18128

**Yang WY, Zheng Y, Bahn SC, Pan XQ, Li MY, Vu HS, Roth MR, Scheu B, Welti R, Hong YY, et al** (2012) The patatin-containing phospholipase A pPLAII$\alpha$ modulates oxylipin formation and water loss in Arabidopsis thaliana. Mol Plant **5:** 452–460

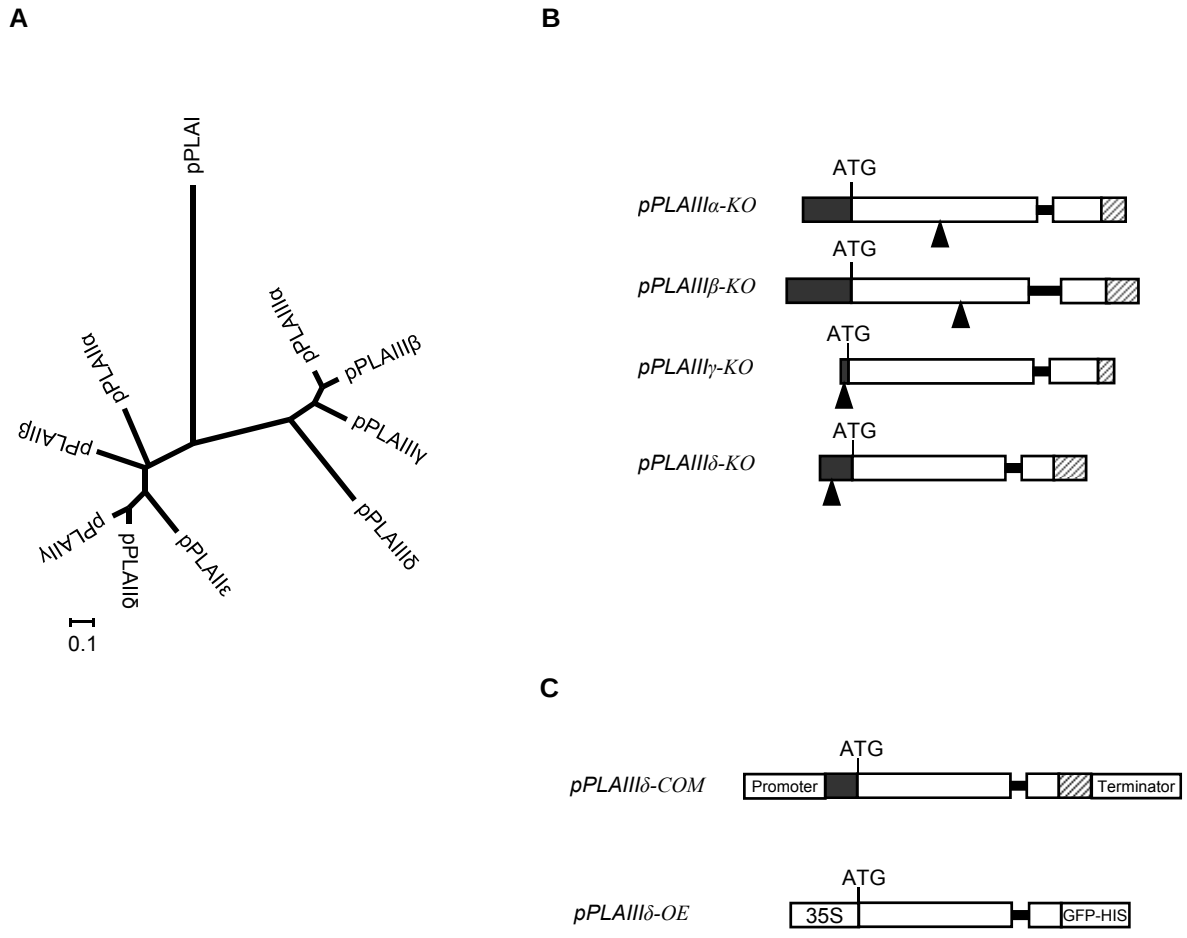


**Supplemental Figure 1. Generation of Knockout, Overexpression, and Complementation Mutants of *pPLAIIIs*.**

(**A**) Phylogenetic tree of the 10 patatin-related phospholipase As (pPLAs) in Arabidopsis generated with MEGA5 (Tamura et al., 2011). The branch lengths of the tree are proportional to divergence. The 0.1 scale represents 10% change.

(**B**) T-DNA insertion sites in the knockout mutants of *pPLAIIIα*, *pPLAIIIβ*, *pPLAIIIγ*, and *pPLAIIIδ*. The arrowhead indicates the position of the T-DNA insertion. The filled boxes, empty boxes, and hatched boxes denote 5'-UTR (untranslated region), exons, and 3'-UTR, respectively. The bold line denotes an intron. The triangles mark the T-DNA insertional sites.

(**C**) Constructs for generating overexpression and complementation mutants of *pPLAIIIδ*. In the *pPLAIIIδ* overexpressors (*pPLAIIIδ-OE*), the Arabidopsis pPLAIIIδ gene was driven by the cauliflower mosaic virus 35S promoter and tagged on the C-terminus with green fluorescence protein and 6xHistidine. In the *pPLAIIIδ* complementation lines (*pPLAIIIδ-COM*), Arabidopsis *pPLAIIIδ* genomic DNA sequence, cloned from promoter to terminator, was transferred into T-DNA of the T-DNA insertional knockout mutant of *pPLAIIIδ*. The empty boxes and filled boxes denote exons and untranslated regions, respectively. Ten independent lines of *pPLAIIIδ-COM* were generated and they were indistinguishable from wild-type. Fifteen independent lines of *pPLAIIIδ-OE* were generated; plans of these OE lines were consistently smaller in plant stature than WT plants.

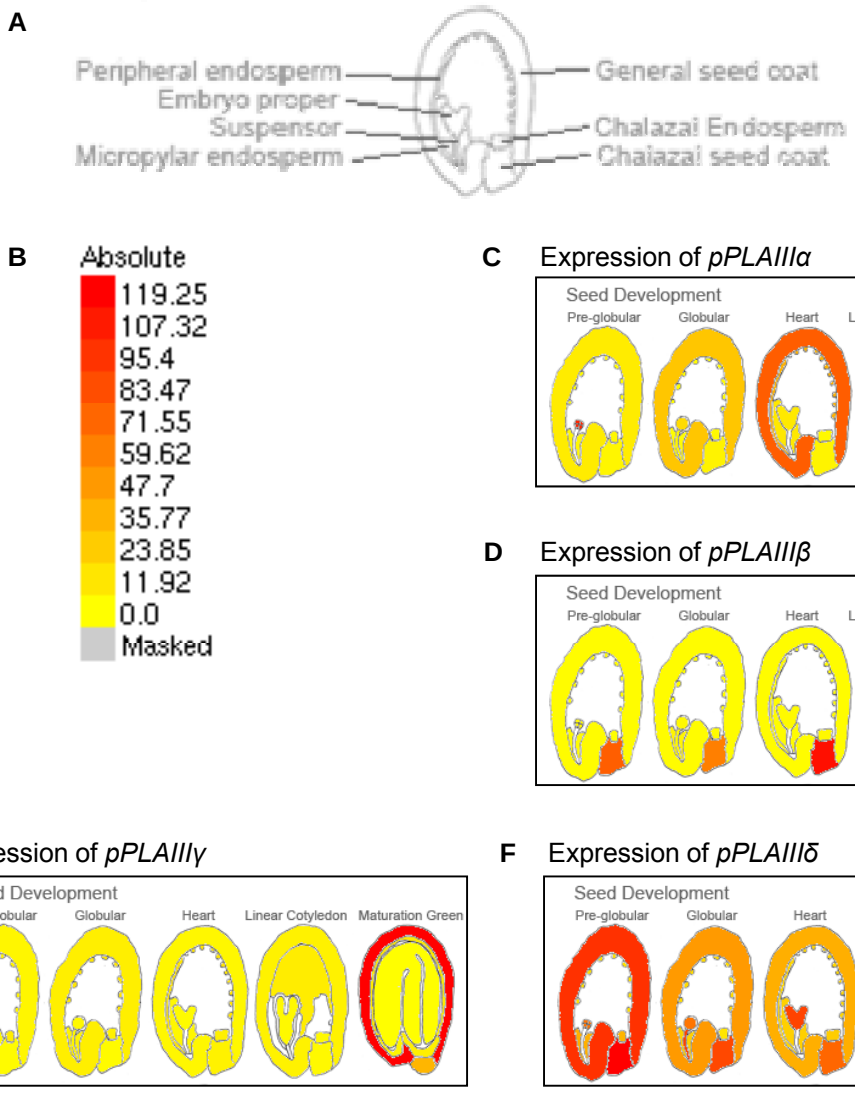


**Supplemental Figure 2. RNA Abundance Patterns of Four pPLAIII Genes in Developing Arabidopsis Seeds.**

The RNA abundance profile of each *pPLAIII* gene was explored with Arabidopsis eFP Browser at bar.utoronto.ca (Winter et al., 2007; Bassel et al., 2008).

(**A**) Diagram showing the tissues of seed coat, endosperm, and embryo in an Arabidopsis developing seed.

(**B**) The magnitude of RNA levels as denoted by coloration in the seed pictographs. The numbers indicate the absolute gene RNA levels.

(**C**) RNA abundance of *pPLAIIIα* in developing Arabidopsis seed. The highest RNA levels were in the general seed coat at the developmental stages heart and linear cotyledon and in endosperm at the developmental stage linear cotyledon.

(**D**) RNA abundance of *pPLAIIIβ* in developing Arabidopsis seed. The highest RNA levels were in chalazal seed coat at the developmental stages heart and linear cotyledon.

(**E**) RNA abundance of *pPLAIIIγ* in developing Arabidopsis seed. The highest RNA level was in the general seed coat at the developmental stage maturation green.

(**F**) RNA abundance of *pPLAIIIδ* in developing Arabidopsis seed. The RNA level was high in developing embryos of all developmental stages. It was high in general seed coat and chalazal seed coat at pre-globular, globular, and heart developmental stages and in the embryo proper at all stages.

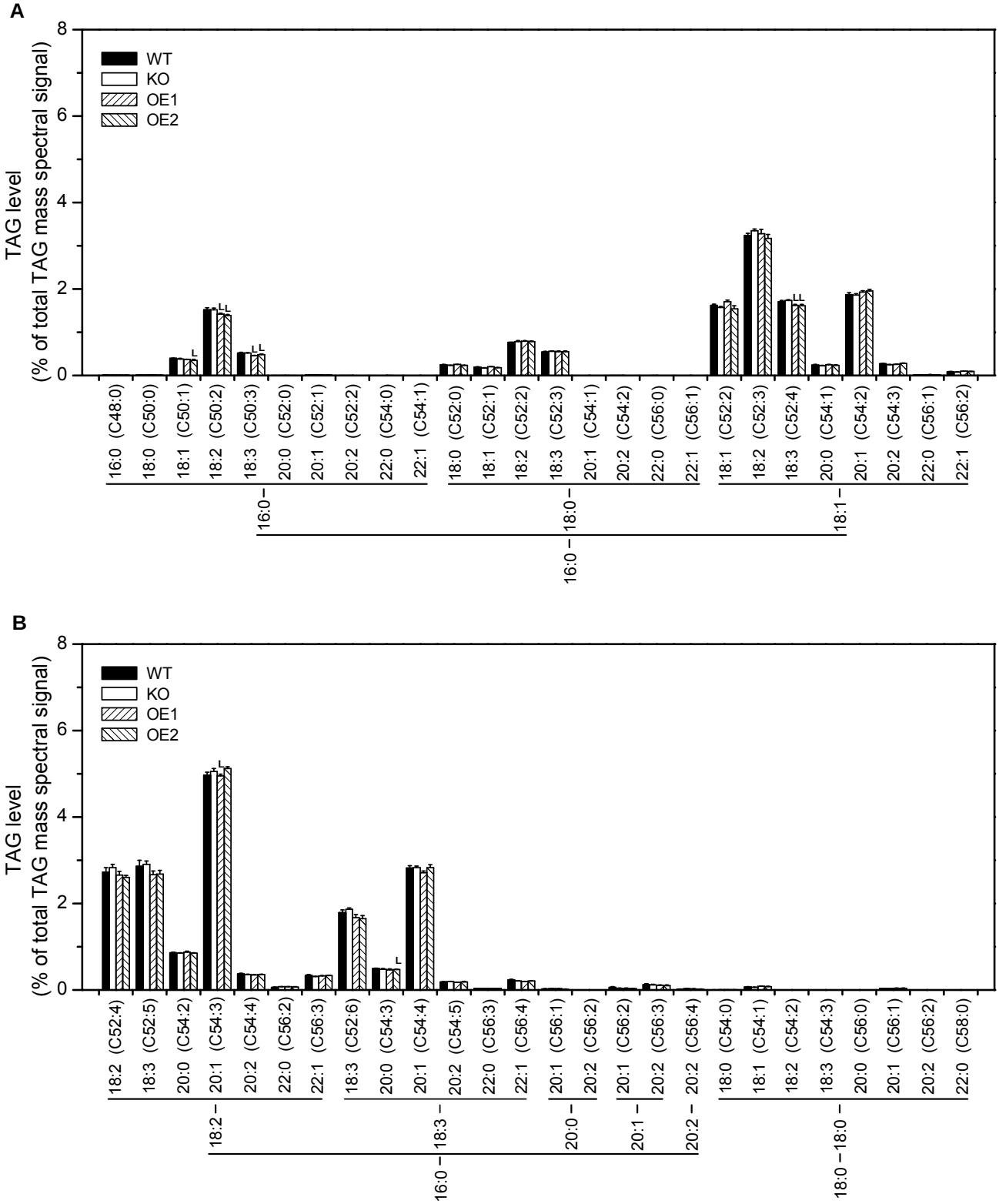


**Supplemental Figure 3**

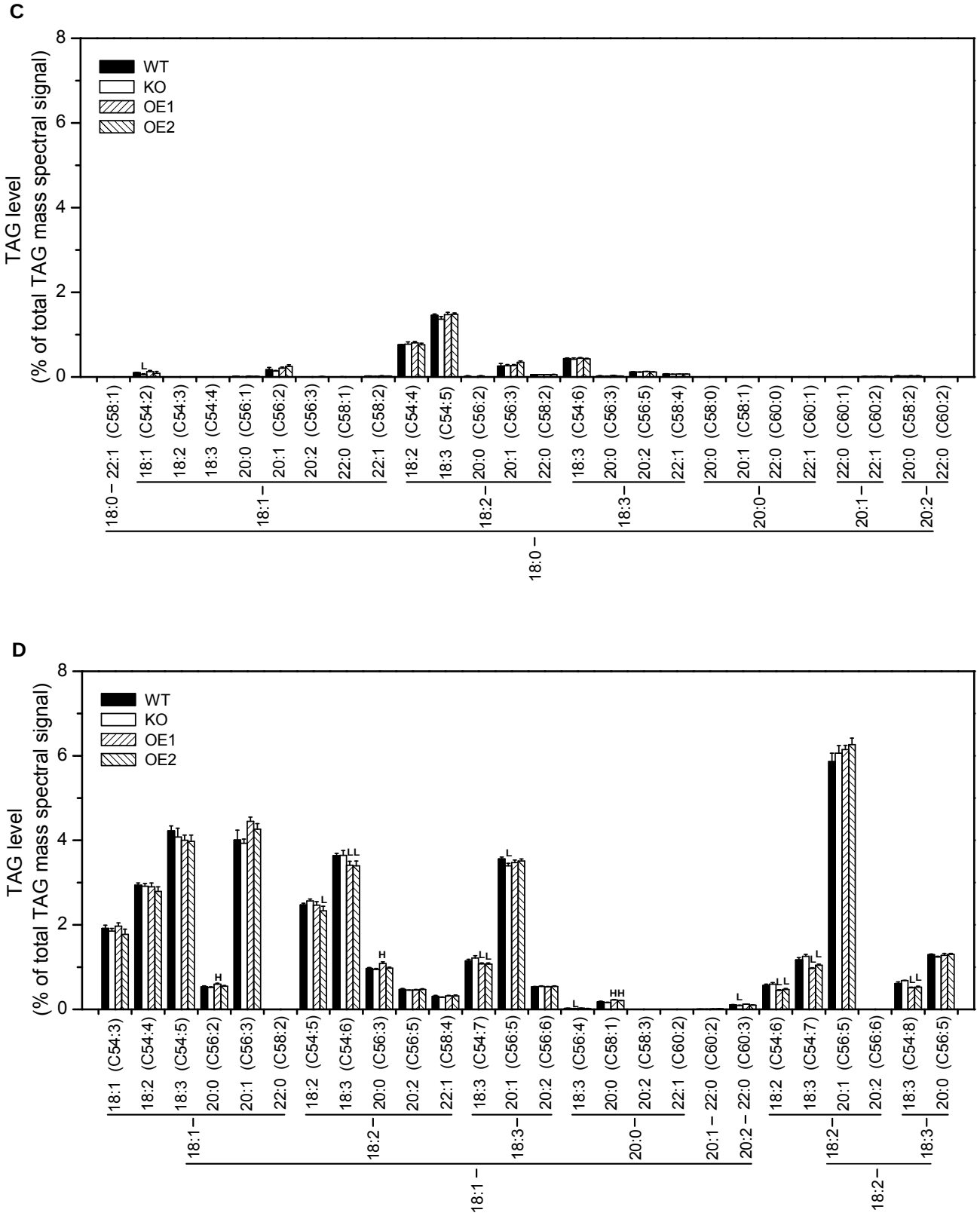


**Supplemental Figure 3**

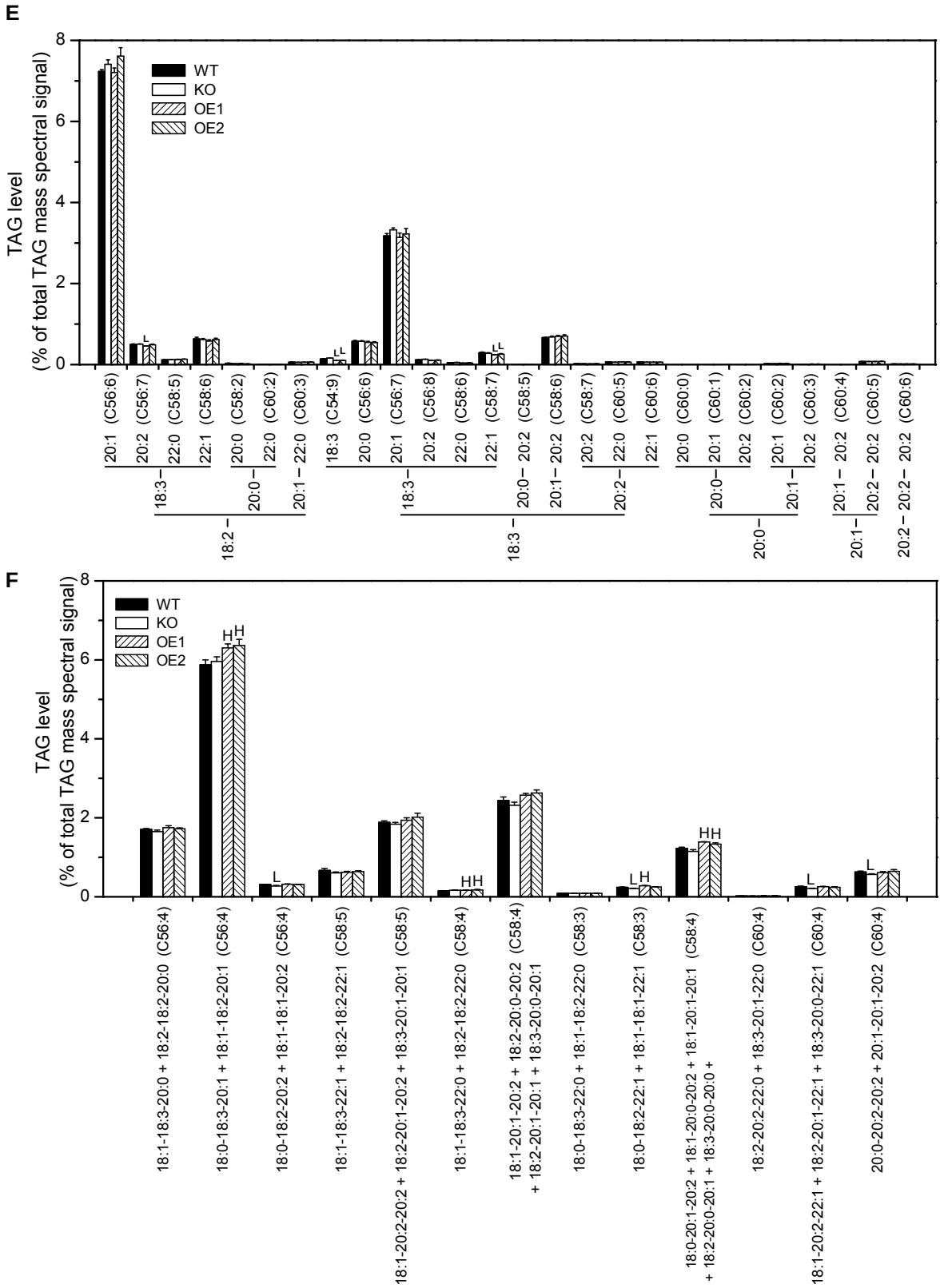


**Supplemental Figure 3. pPLAIIIδ Promotes Increased Levels of 20C Fatty Acyl-containing TAG over 18C Fatty Acyl-containing TAG in Arabidopsis Seeds, as Determined by Mass Spectral Analysis.** Levels of 120 individual (A-E) or grouped (F) TAG species in seeds of WT, KO, and OE mutants. Values are means ± SE (n = 5). $^{H}$Significantly higher and $^{L}$Signifcantly lower, each at $P < 0.05$ compared with the WT, based on Student's *t* test..

**Supplemental Figure 3**

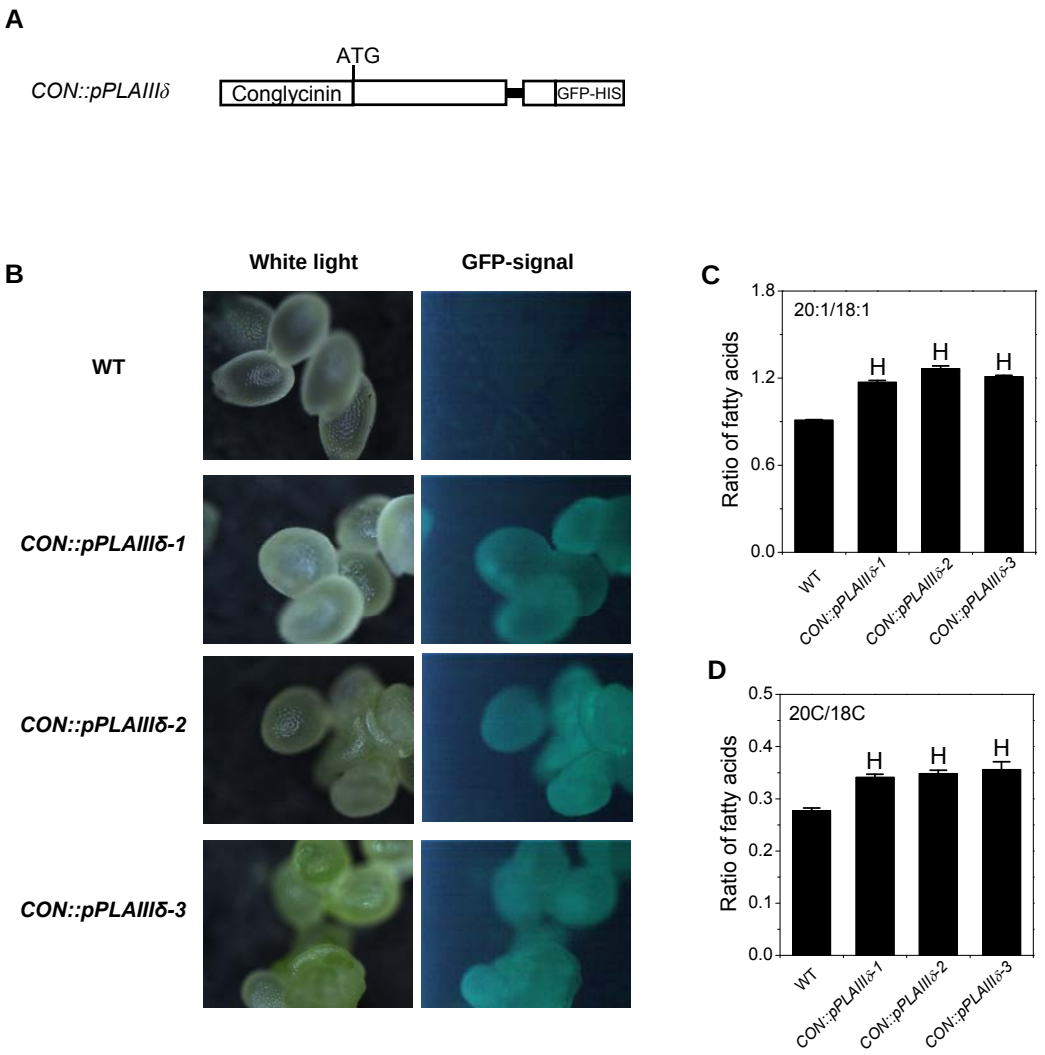


**Supplemental Figure 4. Seed Specific Overexpression of *pPLAIIIδ* in Arabidopsis.**
(**A**) Constructs for generating seed specific expression mutants of pPLAIIIδ. Arabidopsis *pPLAIIIδ* genomic DNA cloned from start codon to stop codon (stop codon removed) was driven by soybean β-conglycinin promoter and tagged on C-terminus by green fluorescence protein and 6xHistidine. The resulting transgenic Arabidopsis were designated as *CON::pPLAIIIδ*. Ten independent lines of T3 generation mutants were obtained. The growth of the *CON::pPLAIIIδ* mutants was comparable with wild-type.
(**B**) Detection of the green fluorescence signal in developing seeds of *CON::pPLAIIIδ* mutants. Developing seeds from Arabidopsis siliques were imaged using a Nikon Eclipse 800 widefield microscope and a X60 differential interference contrast, 1.2-numerical aperture objective, with mercury lamp excitation and a 492/18 BP excitation filter and a 535/40 B emission filter.
(**C**) Ratio of the level of fatty acids of 20:1 over 18:1 in seeds of WT and *CON::pPLAIIIδ* mutants. Values are means ± SE (n = 3). $^{H}$Significantly higher at $P < 0.05$ compared with the WT, based on Student's *t* test.
(**D**) Ratio of the level of fatty acids with 20 carbons over 18 carbons in seeds of WT and *CON::pPLAIIIδ* mutants. Values are means ± SE (n = 3). $^{H}$Significantly higher at $P < 0.05$ compared with the WT, based on Student's *t* test.

**Supplemental Table 1. PCR Primers for Mutant Screening and Molecular Cloning.**

| Gene | AGI | Real time PCR primers |
|---|---|---|
| *pPLAIIIα* | At2g39220 | Screening for T-DNA insertional mutant of Salk_040363:<br>Forward 5'-CCGAGCATCGAGACTGATAAG-3'<br>Reverse 5'-AGTATCAGCTGCTCCATCAGC-3‘<br>T-DNA LB primer 5’-GCGTGGACCGCTTGCTGCAACT-3’ |
| *pPLAIIIβ* | At3g54950 | Screening for T-DNA insertional mutant of Salk_057212:<br>Forward 5'-TTGACGGATATGCAGGAACCAA-3'<br>Reverse 5'-ATGCGTGATTGCAGCCGCTGT-3‘<br>T-DNA LB primer 5’-GCGTGGACCGCTTGCTGCAACT-3’ |
| *pPLAIIIγ* | At4g29800 | Screening for T-DNA insertional mutant of Salk_088404:<br>Forward 5'-GAAAGCTTCCACAATCTAACTG-3'<br>Reverse 5'-GGCGATTCGAGCGTTTGGATC-3‘<br>T-DNA LB primer 5’-GCGTGGACCGCTTGCTGCAACT-3’ |
| *pPLAIIIδ* | At3g63200 | Screening for T-DNA insertional mutant of Salk_029470:<br>Forward 5'-TCGCAGTGAGAGAGCCATTTCT-3'<br>Reverse 5'-CAAGCAACAAATATTAGCTGCCCAAAC-3‘<br>T-DNA LB primer 5’-GCGTGGACCGCTTGCTGCAACT-3’ |
| *pPLAIIIδ* | At3g63200 | Cloning of pPLAIIIδ gene into pEC291 vector for generation of complementation lines:<br>Promoter region primer<br>5'-AGGCGCGCCAAACTATCTCGTGTCGC-3'<br>Terminator region primer<br>5'-AGGCGCGCCACTCTGTGCTGGCTATC-3‘ |
| *pPLAIIIδ* | At3g63200 | Cloning of pPLAIIIδ gene into pMDC83 vector for generation of overexpression lines (35S:: pPLAIIIδ):<br>Forward<br>5'-ATTTAATTAAATGGAGATGGATCTCAGCAAGGTT-3'<br>Reverse<br>5'-ATGGCGCGCCAACGGCCGTCAGCGAGAGGGTTAA-3‘ |
| *pPLAIIIδ* | At3g63200 | Cloning of pPLAIIIδ cDNA into pET28a vector for protein expression in *E. Coli*:<br>Forward<br>5'-TTTGGATCCATGGAGATGGATCTCAGCAAGGTT-3'<br>Reverse 5'-AAGGCGGCCGCACGGCCGTCAGCGAGAGG-3‘ |
| *pPLAIIIδ* | At3g63200 | Cloning of β-conglycinin promoter into pZY101 vector for generation of seed-specific expression lines (CON::pPLAIIIδ):<br>Forward<br>5'-ATGTTTAAACAAGCTTTTGATCCATGCCCTTCAT-3'<br>Reverse<br>5'-ATTTAATTAAGCGGCCGCAGTATATCTTAAATTCT-3‘ |

**Supplemental Table 2. Real time PCR Primers for Quantitative Measurement of Transcript Levels.**

| *Gene* | AGI | Real time PCR primers |
|---|---|---|
| *AAPT1* | At1g13560 | Forward 5'-GCCCTTGGAATCTACTGCTT-3'<br>Reverse 5'-ACATAACTTCACCTATCCTG-3' |
| *AAPT2* | At3g25585 | Forward 5'-CGAACCAAAAGGATTGAAAA-3'<br>Reverse 5'-TCCACAAGAGGAACCCCGTC-3' |
| *CCT1* | At2g32260 | Forward 5'-GCCACTTCTACTAAACTCCC-3'<br>Reverse 5'-CACACACAAACAAACACATC-3' |
| *CCT2* | At4g15130 | Forward 5'-CTGACGATTTCCAAAGACAA-3'<br>Reverse 5'-TTCAATCCCTTTGTTGCTCA-3' |
| *DGAT1* | At2g19450 | Forward 5'-GGTTCATCTTCTGCATTTTCGGA-3'<br>Reverse 5'-TTTTCGGTTCATCAGGTCGTGGT-3' |
| *DGAT2* | At3g51520 | Forward 5'-TGTTTGAGAGGCACAAGTCCCGA-3'<br>Reverse 5'-AGTCCAAATCCAGCTCCAAGGTA-3' |
| *GPAT* | At1g32200 | Forward 5'-CAAGTCGGTGAATGAACAATACG-3'<br>Reverse 5'-TGATTGTGTTTGTGTATCCCTAA-3' |
| *LPAT2* | At3g57650 | Forward 5'-CAAGAACAGAACATTGGCCGTCC-3'<br>Reverse 5'-GCCCAGTGTAGGAACTTTATTGC-3' |
| *LPAT3* | At1g51260 | Forward 5'-ATTTATCACCAAGGATGCTCAAC-3'<br>Reverse 5'-TGAAACCACCGAATACAAGGAAA-3' |
| *LPAT4* | At1g75020 | Forward 5'-CGTTCGGCGAGTTCTACTAAAGG-3'<br>Reverse 5'-TCTTCTTCTGGTCTTTGATTGGG-3' |
| *LPAT5* | At3g18850 | Forward 5'-GATTGCCTTCACCACCATCTGTA-3'<br>Reverse 5'-AGCAGAGGTCAAGTAGACACAGG-3' |
| *LPCAT1* | At1g63050 | Forward 5'-TGCGGTTCAGATTCCGCTTTTCT-3'<br>Reverse 5'-GTTGCCACCGGTAAATAGCTTTCG-3' |
| *PAH1* | At3g09560 | Forward 5'-ACCCGTTCTATGCCGGATTTGG-3'<br>Reverse 5'-TCCTGTTGCCACTTCTCCCTTTG-3' |
| *PDAT1* | At5g13640 | Forward 5'-GGAGTGGGGATACCAACGGAACG-3'<br>Reverse 5'-GAAAGGGGATGCAACTGTCGGGA-3' |
| *pPLAIIIα* | At2g39220 | Forward 5'-GTAGCAGAGGAGATGCTGAAGCAGAA-3'<br>Reverse 5'-TACAGTGGGAGCGATTCTACAACTCC-3' |
| *pPLAIIIγ* | At4g29800 | Forward 5'-CACGGATCCAAGAGCAGAGAATGTGA-3'<br>Reverse 5'-CTAACACTTCGTCGCTGCTGCTCAAT-3' |
| *pPLAIIIδ* | At3g63200 | Forward 5'-CAACGTCTTGTTGCGTCAGGAAAGTC-3'<br>Reverse 5'-ATTAACTCGAAGATGCTGGCTGGG-3' |
| *UBQ10* | At4g05320 | Forward 5'-CACACTCCACTTGGTCTTGCGT-3'<br>Reverse 5'-TGGTCTTTCCGGTGAGAGTCTTCA-3' |

**SUPPORTING INFORMATION**

**Supplemental Figure 1. Generation of Knockout, Overexpression, and Complementation Mutants of *pPLAIIIs*.**

(**A**) Phylogenetic tree of the 10 patatin-related phospholipase As (pPLAs) in Arabidopsis generated with MEGA5 (Tamura et al., 2011). The branch lengths of the tree are proportional to divergence. The 0.1 scale represents 10% change.

(**B**) T-DNA insertion sites in the knockout mutants of *pPLAIIIα*, *pPLAIIIβ*, *pPLAIIIγ*, and *pPLAIIIδ*. The arrowhead indicates the position of the T-DNA insertion. The filled boxes, empty boxes, and hatched boxes denote 5'-UTR (untranslated region), exons, and 3'-UTR, respectively. The bold line denotes an intron.

(**C**) Constructs for generating overexpression and complementation mutants of *pPLAIIIδ*. In the *pPLAIIIδ* overexpressors (*pPLAIIIδ-OE*), the Arabidopsis pPLAIIIδ gene was driven by the cauliflower mosaic virus 35S promoter and tagged on the C-terminus with green fluorescence protein and 6xHistidine. In the *pPLAIIIδ* complementation lines (*pPLAIIIδ-COM*), Arabidopsis *pPLAIIIδ* genomic DNA sequence, cloned from promoter to terminator, was transferred into T-DNA of the T-DNA insertional knockout mutant of *pPLAIIIδ*. The empty boxes and filled boxes denote exons and untranslated regions, respectively. Ten independent lines of *pPLAIIIδ-COM* were generated and they were indistinguishable from wild-type. Fifteen independent lines of *pPLAIIIδ-OE* were generated; plans of these OE lines were consistently smaller in plant stature than WT plants.

**Supplemental Figure 2. Transcript Accumulation Patterns of Four pPLAIII Genes in Developing Arabidopsis Seeds.**

The mRNA accumulation profile of each *pPLAIII* gene was explored with Arabidopsis eFP Browser at bar.utoronto.ca (Winter et al., 2007; Bassel et al., 2008).

(**A**) Diagram showing the tissues of seed coat, endosperm, and embryo in an Arabidopsis developing seed.

(**B**) The magnitude of RNA levels as denoted by coloration in the seed pictographs. The numbers indicate the absolute RNA levels.

(**C**) RNA levels of *pPLAIIIα* in developing Arabidopsis seed. The highest RNA levels were in the general seed coat at the developmental stages heart and linear cotyledon and in endosperm at the developmental stage linear cotyledon.
(**D**) RNA levels of *pPLAIIIβ* in developing Arabidopsis seed. The highest RNA levels were in chalazal seed coat at the developmental stages heart and linear cotyledon.
(**E**) RNA levels of *pPLAIIIγ* in developing Arabidopsis seed. The highest RNA level was in the general seed coat at the developmental stage maturation green.
(**F**) RNA level of *pPLAIIIδ* in developing Arabidopsis seed. The RNA level was high in developing embryos of all developmental stages. It was high in general seed coat and chalazal seed coat at pre-globular, globular, and heart developmental stages and in the embryo proper at all stages.

**Supplemental Figure 3. pPLAIIIδ Promotes Increased Levels of 20C Fatty Acyl-containing TAG over 18C Fatty Acyl-containing TAG in Arabidopsis Seeds, as Determined by Mass Spectral Analysis.**

Levels of 120 individual (A-E) or grouped (F) TAG species in seeds of WT, KO, and OE mutants. Values are means ± SE (n = 5). $^{H}$Significantly higher and $^{L}$Signifcantly lower, each at $P < 0.05$ compared with the WT, based on Student's *t* test.

**Supplemental Figure 4. Seed Specific Overexpression of *pPLAIIIδ* in Arabidopsis.**

(**A**) Constructs for generating seed specific expression mutants of pPLAIIIδ. Arabidopsis *pPLAIIIδ* genomic DNA cloned from start codon to stop codon (stop codon removed) was driven by soybean β-conglycinin promoter and tagged on C-terminus by green fluorescence protein and 6xHistidine. The resulting transgenic Arabidopsis were designated as *CON::pPLAIIIδ*. Ten independent lines of T3 generation mutants were obtained. The growth of the *CON::pPLAIIIδ* mutants was comparable with wild-type.
(**B**) Detection of the green fluorescence signal in developing seeds of *CON::pPLAIIIδ* mutants. Developing seeds from Arabidopsis siliques were imaged using a Nikon Eclipse 800 widefield microscope and a X60 differential interference contrast, 1.2-numerical aperture objective, with mercury lamp excitation and a 492/18 BP excitation filter and a 535/40 B emission filter.

(**C**) Ratio of the level of fatty acids with 20 carbons over 18 carbons in seeds of WT and *CON::pPLAIIIδ* mutants. Values are means ± SE (n = 3). [H]Significantly higher at $P < 0.05$ compared with the WT, based on Student's *t* test.

(**D**) Ratio of the level of fatty acids of 20:1 over 18:1 in seeds of WT and *CON::pPLAIIIδ* mutants. Values are means ± SE (n = 3). [H]Significantly higher at $P < 0.05$ compared with the WT, based on Student's *t* test.

**Supplemental Table 1. PCR Primers for Mutant Screening and Molecular Cloning.**

**Supplemental Table 2. Real Time PCR Primers for Quantitative Measurement of Transcript Levels.**

**Supplemental Method 1. Mass Spectral Analysis of TAG**

An automated, direct-infusion electrospray ionization-tandem mass spectrometry approach was used for TAG analysis. A precise amount of internal standard (0.5 nmol tri17:1-TAG, Avanti Polar Lipids) was added to around 25 mg of dry Arabidopsis seeds, which were ground with mortar and pestle in 1.0 mL of chloroform/methanol (2:1). The mixture were extracted with shaking for 1 h at room temperature and centrifuged to pellet the debris. Fifty microliters of the supernatant were combined with 310 μL chloroform, and 840 μL of chloroform/methanol/300 mM ammonium acetate in water (300:665:35). The final volume was 1.2 mL.

Unfractionated lipid extracts were introduced by continuous infusion into the ESI source on a triple quadruple MS (API4000, Applied Biosystems, Foster City, CA). Samples were introduced using an autosampler (LC Mini PAL, CTC Analytics AG, Zwingen, Switzerland) fitted with the required injection loop for the acquisition time and presented to the ESI needle at 30 l/min. TAGs were detected by a series of neutral loss scans that detected TAG species as $[M + NH_4]^+$ ions. The scans targeted losses of various fatty acids as neutral ammoniated fragments: NL 285.2 (17:1, for the TAG internal standard); NL 273.2 (16:0); NL 301.2 (18:0); NL 299.2 (18:1); NL 297.2 (18:2); NL 295.2 (18:3); NL 329.2 (20:0); NL 327.2 (20:1); NL 325.2 (20:2); NL 357.2 (22:0); NL 355.2 (22:1). The scan speed was 100 u per sec. The collision energy, with nitrogen in the collision cell, was +20 V, declustering potential was +100 V, entrance potential

was +14 V, and exit potential was +14 V. Sixty continuum scans were averaged in MCA mode (multiple channel analyzers).

For all analyses the collision gas pressure was set on "low", and the mass analyzers were adjusted to a resolution of 0.7 u full width at half height. The source temperature (heated nebulizer) was 100°C, the interface heater was on, +5.5 kV was applied to the electrospray capillary, the curtain gas was set at 20 (arbitrary units), and the two ion source gases were set at 45 (arbitrary units).

For TAG analyses, the background of each spectrum was subtracted, the data were smoothed, and peak areas integrated using a custom script and Applied Biosystems Analyst software. Peaks corresponding to the target lipids in these spectra were identified, and the data were corrected for A+2 isotopic overlap (based on the *m/z* of the charged fragments) within each spectra. Signals were also corrected for isotopic overlap across spectra, based on the A+2 overlaps and masses of the neutral fragments. All signals for each sample were normalized to the signal of the internal standard. A sample containing internal standard alone, run through the same series of scans, was used to correct for chemical or instrumental noise: amounts of each target lipid detected in the ''internal standards-only''sample were subtracted from the molar amounts of each target lipid calculated from the plant lipid spectra. The ''internal standards-only'' spectra were used to correct the data from the following five samples run on the instrument.

The corrected data from all fatty acyl (NL) scans for each TAG species, as defined by *m/z*, which corresponds to total acyl carbons: total double bonds (e.g. 52:3), were used to calculate the amount of each individual TAG species. As described by Han and Gross, formulas were developed to assign particular signals from the NL scans to particular TAGs (Han and Gross, 2001). Once values for all TAGs were calculated, the amount of each TAG was expressed as a percentage of the total values for all TAG species. Because there is variation in ionization efficiency among acyl glycerol species with different fatty acyl groups (Han and Gross, 2001) and, here, no response factors for individual species were determined, the values are not directly proportional to the TAG content of each species. However, the amounts of particular TAG species can be meaningfully compared across samples.